Paleoceanography and Paleoclimatology

RESEARCH ARTICLE
10.1029/2020PA003986

Key Points:

- Benthic foraminiferal faunas indicate dysoxia was more severe than in the modern Gulf of Alaska during the Bølling-Allerød and MIS 3
- Changes in oxygenation can exceed 1 ml/L O_2 per 100 years and dysoxic conditions persist for <300 to ~4,000 years
- The frequency and timing of low-oxygen events in the Gulf of Alaska are similar to lower latitudes in the North Pacific

Supporting Information:

- Supporting Information S1
- Table S1
- Table S2
- Table S3
- Table S4
- Table S5
- Table S6

Correspondence to:
C. Belanger,
Christina.Belanger@tamu.edu

Citation:
Sharon, Belanger, C., Du, J., & Mix, A. (2021). Reconstructing paleo-oxygenation for the last 54,000 years in the Gulf of Alaska using cross-validated benthic foraminiferal and geochemical records. *Paleoceanography and Paleoclimatology*, *36*, e2020PA003986. https://doi.org/10.1029/2020PA003986

Received 24 MAY 2020
Accepted 23 DEC 2020

Reconstructing Paleo-oxygenation for the Last 54,000 Years in the Gulf of Alaska Using Cross-validated Benthic Foraminiferal and Geochemical Records

Sharon[1], Christina Belanger[1], Jianghui Du[2,3], and Alan Mix[2]

[1]Department of Geology and Geophysics, Texas A&M University, College Station, TX, USA, [2]College of Earth, Ocean, and Atmospheric Sciences, Oregon State University, Corvallis, OR, USA, [3]Department of Earth Sciences, Now at Institute of Geochemistry and Petrology, ETH Zürich, Zürich, Switzerland

Abstract Holocene and Pleistocene marine sediment records in the North Pacific record multiple dysoxic events proximal to continental margins and oxygen minimum zones (OMZs). High-resolution paleoenvironmental studies in the Gulf of Alaska (GoA) were previously restricted to the last ~17,000 years, limiting our knowledge of oxygenation in the high latitude North Pacific. Here we develop a ~54,000-year-long record of co-registered benthic foraminiferal assemblages and redox sensitive metal concentrations (Mo/Al and U/Al) at Site U1419 in the upper OMZ of GoA to reconstruct the history of OMZ extent and intensity at multi-centennial resolution. Using multivariate analyses of total benthic foraminiferal assemblages, we develop quantitative dissolved oxygen estimates that are robust to differences in the benthic foraminiferal size fraction analyzed, replicate modern oxygenation patterns in the GoA, and are cross-validated by redox sensitive metal concentrations. We identify dysoxic events in the early Holocene and in the Bølling-Allerød (B/A), consistent with previous studies, as well as two dysoxic events during MIS 3 that are comparable in severity to the B/A event and lower in oxygen than the modern GoA OMZ. We further record short-duration (<300 years) dysoxic events during glacial times similar to those recorded at more southern latitudes. Rates of oxygenation change can be abrupt with transitions exceeding 1 ml/L O_2 in 100 years. Quantitative estimates of paleo-oxygenation, such as those possible with benthic foraminiferal assemblages, are important for forecasting future oxygenation changes in OMZs and their potential impacts on the marine ecosystems.

1. Introduction

Low-oxygen conditions occur naturally in fjords, upwelling zones, restricted basins, and at intermediate ocean depths within oxygen minimum zones (OMZs). The intensity and spatial extent of OMZs vary with changes in global climate, ocean circulation, and nutrient availability (Deutsch et al., 2011; Helly & Levin, 2004; Keeling et al., 2010). Since at least the 1960s, the global ocean oxygen inventory has declined, including within OMZ cores, and upper OMZ boundaries have shoaled (Bograd et al., 2008; Ito et al., 2017; Pierce et al., 2012; Schmidtko et al., 2017; Whitney et al., 2007). This expansion and intensification of OMZs are a major threat to ecosystem health (Diaz & Rosenberg, 2008; Gilly et al., 2013; Helly & Levin, 2004). In addition, changes in OMZ size and extent affect nutrient and carbon cycle processes with particular effects on deep-sea carbon storage with global climate consequences (Gray et al., 2018; Keeling et al., 2010).

The North Pacific contains the most extensive modern OMZ and the lowest minimum oxygen values in the ocean due to the longer circulation paths (Paulmier & Ruiz-Pino, 2009). North Pacific paleoceanographic records document changes in the extent of its OMZs since the Late Pleistocene including sites in Baja California, the California Margin, Santa Barbara Basin (SBB), East and South China Seas, Sea of Japan, Sea of Okhotsk, Bering Sea, the Cascadia Margin, and the southeastern margin of Alaska (Belanger et al., 2020; Bubenshchikova et al., 2015; Cartapanis et al., 2011; Davies et al., 2011; K. Cannariato & Kennett, 1999; K. G. Cannariato et al., 1999; K. Ohkushi et al., 2013; Li et al., 2018; McKay et al., 2005; Mix et al., 1999; Moffitt et al., 2014; Praetorius et al., 2015; Saravanan et al., 2020; Shibahara et al., 2007; Takahashi et al., 2016; Tetard et al., 2017; Zou et al., 2020). In many of these records, low-oxygen events correspond to warmer periods, such as the Bølling-Allerød (B/A) and interstadials during glacial conditions. Proposed proximal drivers of deoxygenation during these events include decreased oxygen solubility directly related to warming,

enhanced productivity, and thus respiration, due to changes in nutrient supply, and decreased intermediate water ventilation (Gray et al., 2018; Jaccard & Galbraith, 2012; Moffitt et al., 2015; Praetorius et al., 2015).

Previous studies of low-oxygen events in the southeastern margin of Alaska are restricted to the last ~17,000 years (Addison et al., 2012; Davies et al., 2011; Praetorius et al., 2015). These paleoceanographic records suggest OMZ expansion and strengthening in the Gulf of Alaska (GoA) during B/A interstadial (14.7–12.9 ka) and the early Holocene; 11.5–10.5 ka. However, the frequency and severity of hypoxia for glacial intervals are not documented for this region as they have been elsewhere in the North Pacific. This paleoceanographic gap in the high-latitude North Pacific is largely due to poor preservation of microfossils in corrosive bottom waters. Paleoceanographic records for the past ~54,000 years are obtainable in the GoA, though, due to high sedimentation rates that led to the excellent preservation of foraminifera (Gulick et al., 2015).

Combined sedimentary, faunal, and geochemical approaches are important for resolving oxygenation records because each proxy has limitations. The presence of laminations indicates the absence of bioturbation due to severe low-oxygen conditions (Moffitt et al., 2015; van Geen et al., 2003). However, these sedimentary structures are easily overprinted by later bioturbation when oxic conditions return, especially if sedimentation rates are low. Redox-sensitive metal accumulations (including Mo and U) are instrumental in reconstructing dysoxia (<0.5 ml/L O_2), including in the North Pacific (Davies et al., 2011; Jaccard & Galbraith, 2013; Moffitt et al., 2015; Praetorius et al., 2015; Zheng et al., 2002). However, processes like post-diagenetic reworking, re-oxidative burn down, bioturbation, sedimentary dilution, and diffusion within the sediments can overprint oxygenation histories based on redox-sensitive metals (Calvert & Pedersen, 1993; Tribovillard et al., 2006; Zindorf et al., 2020). This may lead to imprecise interpretations of paleoenvironmental conditions like the severity, duration, and timing of the events.

Benthic foraminifera are particularly useful for studying oxygenation because some species rapidly respond to changes in oxygenation but are insensitive to oxygenation differences above 1 or 2 ml/L (McCune et al., 2002; Moffitt et al., 2015). Like sedimentary proxies, bioturbation can mix foraminifera accumulated under different environmental conditions across environmental changes leading to time-averaged assemblages in the sediment core (Fürsich & Aberhan, 1990). This time-averaging can dampen the signal of low-oxygen events but, unlike redox-sensitive metals, foraminifera are not necessarily removed from the sediments. However, many environmental factors can influence the distribution of benthic foraminifera including organic carbon flux, salinity, current velocity, temperature, and substrate characteristics, and thus, can confound paleo-oxygen reconstruction, especially when based on only a few index species (Jorissen et al., 2007). Thus, cross-validation across sedimentary, faunal, and geochemical proxies is important for reconstructing paleo-oxygenation.

Like index taxon approaches, paleoenvironmental reconstructions based on benthic foraminifera restricted to larger (>125 μm) sizes may also exclude species and overlook some environmental information, especially in low-oxygen or eutrophic environments (Schönfeld et al., 2012; Schroeder et al., 1987; Sen Gupta et al., 1987; Weinkauf & Milker, 2018). However, separating smaller foraminifera from sediments is time-intensive and they are more difficult to identify thus, some studies exclude them for efficiency (Schroeder et al., 1987; Weinkauf & Milker, 2018). Therefore, we must also consider the sensitivity of foraminiferal assemblage-based paleo-oxygenation proxies to taxonomic and size inclusion.

In this study, we use both benthic foraminiferal assemblages and redox sensitive metals as proxies for pore-water oxygenation and assess their correspondence in reconstructing a quantitative oxygenation history of the upper OMZ in GoA. We develop a new method for calculating oxygenation values from total benthic foraminiferal assemblages, which is not limited to taxa with known physiological tolerances. Further, we examine the influence of faunal size-fraction on this correspondence and on the resulting paleoxygenation reconstructions. With these data, we reconstruct an oxygenation history over the last ~54,000 years at ~200-year resolution to test the hypotheses that: a) hypoxia occurred in both glacial and interglacial intervals in the GoA, b) the duration and severity of hypoxia are independent of whether the event occurred during glacial or interglacial times, and c) ecologically relevant changes in oxygenation can occur on multi-centennial timescales in GoA.

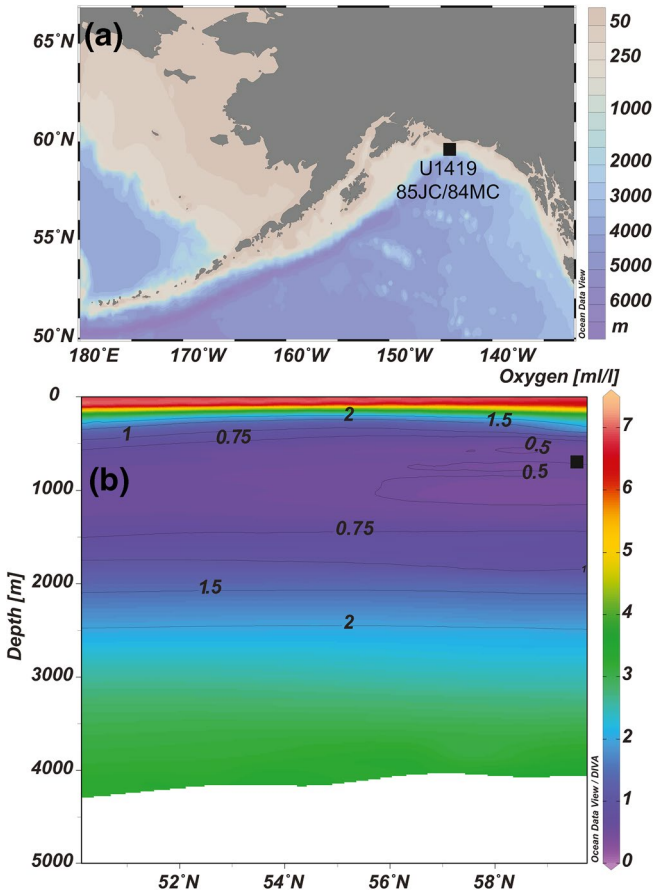

Figure 1. Study site locations. (a) Map showing the location of sites EW0408-85JC, EW0408-84MC, and Site U1419 in the Gulf of Alaska. (b) Meridional cross section (144°W) of the oxygen concentration in the modern Eastern Pacific Ocean, showing location of site with respect to the OMZ. Oxygenation data are from the World Ocean Atlas 2013 (Garcia et al., 2013) and both panels were constructed in Ocean Data View (Schlitzer, 2018). OMZ, oxygen minimum zone.

2. Materials and Methods

Integrated Ocean Drilling Program (IODP) Site U1419, jumbo piston core EW0408-85JC and an adjacent multicore EW0408-84MC are located on the Khitrov Bank in the GoA at 697 and 682 m water depth, respectively, and underlie North Pacific Intermediate Water (NPIW; Figure 1; Jaeger et al., 2014). The modern OMZ core in GoA is at ~670–1,060 m (~0.45 ml/L O_2; Paulmier & Ruiz-Pino, 2009), thus this site lies within the upper OMZ. The central GoA is a high nutrient low chlorophyll area and micronutrients, like iron, limit productivity (Stabeno et al., 2004). Nitrates and phosphates are generally transported from the subsurface ocean (Childers et al., 2005), while iron comes from fluvial sources (Stabeno et al., 2004). The availability of sunlight is the main limiting factor for the primary productivity in the GoA, and productivity is low in winters and comparatively high in early summer (Stabeno et al., 2004). Early spring may have large algal blooms due to availability of ample sunlight and nutrients (Stabeno et al., 2004).

Site U1419 was drilled to ~177 m below the seafloor with an overall core recovery of 82% (Jaeger et al., 2014). The chronology for Site U1419 is based on a Bayesian age model using 250 ^{14}C values from separately analyzed benthic and planktonic foraminiferal samples that were calibrated using the Marine13 calibration curve (Walczak et al., 2020). The base of the stratigraphic splice among holes at U1419 is ~55 ka. Sedimentation rates at Site U1419 average ~50 cm/ka over the past 12 ka, are as high as 800 cm/ka during the deglacial interval, and average ~200 cm/ka during the glacial portion of the record (Walczak et al., 2020). These high sedimentation rates led to exceptional preservation of carbonate, including foraminiferal fossils (Gulick et al., 2015).

The width of the continental shelf in SE Alaska is ~25 km near Kayak Island with shelf break at 220 m water depth (Dobson et al., 1998; Molnia, 1983). As a result, lithology in the continental shelf varies from hemipelagic muds to glacial diamictites, and glacial-marine sand and silt (Carlson, 1989; Penkrot et al., 2018). The dominant lithofacies recorded in the Site U1419 core is clast poor diamict, and facies ranged from massive bioturbated mud to laminated diamicts (Penkrot et al., 2018). Laminations occur during the deglacial, similar to site survey core EW0408-85JC (Davies et al., 2011), but also within the glacial interval (Penkrot et al., 2018).

We sampled 2 to 3-cm-wide intervals (5–40 cc) with a median age resolution of 127 years (interquartile range [IQR] = 73–201 years) based upon the age model from Walczak et al. (2020). Sample ages and depths are calculated from the midpoint of sample width. Approximately 2 cc of each sample was reserved for redox metals analyses and the remainder was disaggregated for faunal analyses.

2.1. Multivariate Faunal Analysis

Sediment samples for faunal analysis were weighed after freeze-drying, disaggregated in deionized water, and wet-sieved at 63 μm. After air-drying, the coarse fraction (>63 μm) was weighed and used to calculate the proportion of sand and silt. Coarse fractions were split with a microsplitter to obtain at least 150 benthic foraminifera specimens >63 μm in each sample. Samples with a high proportion of sand-sized sediment grains often had fewer specimens due to sedimentary dilution and samples with as few as 50 individuals in the >63 μm fraction were retained for analysis. The median number of individuals we obtained per sample is 268 (IQR = 159–404). While previous work estimates 300 individuals are needed for statistical analyses

Table 1
Comparison of Ecological Analyses on Benthic Foraminiferal Assemblages Using Three Size Fractions (>63 μm, >125 μm, and 63–125 μm)

Size fraction used	>63 μm	>125 μm	63–125 μm
Total number of taxa	74	67	67
Number of taxa used in analyses (>2%)	48	46	47
Median number of individuals per sample (Interquartile Range; IQR)	268 (159–404)	81 (46–141)	175 (85–265)
DCA Axis 1, proportion of variance summarized	55%	51%	52%
DCA Axis 2, proportion of variance summarized	16%	6%	19%
Spearman rho DCA 1 versus Mo/Al	0.45 (0.35–0.55)***	0.45 (0.35–0.54)***	0.43 (0.33–0.53)***
Spearman rho CA 1 versus U/Al	0.61 (0.54–0.69)***	0.58 (0.50–0.66)***	0.59 (0.51–0.66)***
Spearman rho DCA 2 versus Mo/Al	−0.33 (−0.42 to 0.25)***	0.01 (−0.10 to 0.12)ns	−0.06 (−0.17 to 0.04)ns
Spearman rho DCA 2 versus U/Al	−0.14 (−0.23 to −0.04)*	0.28 (0.18–0.37)***	−0.18 (−0.29 to −0.08)***
Mantel correlation Faunal versus Mo, U dissimilarity	0.47 (0.46–0.49)**	0.42 (0.41–0.43)**	0.39 (0.38–0.41)**

Note. For Spearman correlations, rho-values are reported; for Mantel correlations, *r*-values are reported. 95% confidence intervals for each correlation are in parentheses.
*$p < 0.05$; **$p < 0.01$, ***$p < 0.001$, ns = non-significant.

of diversity metrics (Buzas, 1990), more recent studies suggest that multivariate analyses of assemblage composition are stable with as few as 58 individuals (Forcino et al., 2015). Foraminifera were picked and identified to species-level within four size fractions (>355 μm, 355–250 μm, 125–250 μm, and 63–125 μm) to retain size information (Table S1). Species that were rare and occurred infrequently were often grouped at the genus-level for counts. Only those species and generic groups that occurred in more than one sample and comprised >2% of individuals in at least one sample were included in analyses.

We use the multivariate ordination method detrended correspondence analysis (DCA) to reduce the dimensionality of our faunal data set and extract major gradients in faunal composition. DCA, which uses the chi-square dissimilarity among the relative abundances of taxa to define assemblage differences, is commonly used in paleoecological analyses and is preferred when the research emphasis is on finding a single faunal gradient reflective of environmental gradients (Belanger & Villarosa Garcia, 2014; Bush & Brame, 2010; McCune et al., 2002; Scarponi & Kowalewski, 2004). We then test the hypothesis that oxygenation influences the primary axes of faunal variation by comparing by DCA species scores of taxa with different environmental preferences in the modern (Table S2). DCA analyses are performed using the "decorana" function with its defaults in vegan package of the R programming language (Oksanen et al., 2017; R Core Team, 2016). We calculate the proportion of variance summarized by each axis using the Pearson correlation between the Euclidean dissimilarity of the DCA sites scores and the Bray-Curtis dissimilarity of the faunal abundances for each site with the *mantel* function in the "ecodist" package ("after the fact method" of McCune et al., 2002).

To test the hypothesis that different benthic foraminiferal size fractions reconstruct the same environmental gradients, we perform DCA analyses on three size fractions (>63 μm, >125 μm, and 63–125 μm) separately. Subsetting the data by size fraction necessarily reduces the number of individuals per sample, thus, these analyses contain samples with fewer than the typically recommended 300 to 58 individuals per sample (Table 1). We do not perform DCA analyses using subsets focused on the larger size fractions alone because we obtained fewer than 50 individuals larger than 250 μm in ~90% of samples (median = 12 individuals >250 μm). We use the Mantel correlation among sample ordination scores to test whether the resulting ordination structures are significantly different. Similarly, we use the Mantel test to compare the similarity

of species positions in ordination space. Mantel tests were performed using *mantel* function in the "ecodist" package in R (Goslee & Urban, 2007).

2.2. Redox Sensitive Metals

Authigenic accumulations of Molybdenum (Mo) and Uranium (U) are commonly used as paleo-oxygen proxies. In sulfidic environments, Mo solubility decreases, thus the concentration of authigenic Mo can serve as a geochemical tracer of severely dysoxic (<0.5 ml/L O_2) conditions (Crusius et al., 1996; McManus et al., 2006; Zheng et al., 2000). Accumulation of authigenic U in sediments typically occurs at similar redox condition as the reduction of iron oxyhydroxides and thus indicates less severe, suboxic (<1.4 ml/L O_2) conditions (Klinkhammer & Palmer, 1991; McManus et al., 2006; Tribovillard et al., 2006). Thus, when used together, U and Mo allow differentiation of suboxic and sulfidic conditions respectively, increasing the quantifiably of paleo-oxygen reconstructions.

Mo and U were measured in bulk sediment samples (~50–100 mg) and digested using a mixture of HF-HCl-HNO_3 in a CEM MARS-6 microwave oven (J. M. Muratli et al., 2012). Mo and U concentrations were analyzed on a quadrupole ICP-MS in the W.M. Keck Collaboratory for Plasma Spectrometry of Oregon State University. Samples, calibration standards, and blanks were spiked with internal standards (^{103}Rh and ^{209}Bi). Procedural blanks of the entire process were corrected for and were 0.8 ± 0.3 (1σ) % for Mo and 0.03 ± 0.01 (1σ) % for U. Repeated analysis of sediment reference material PACS-2 produced a Mo concentration of 5.70 ± 0.23 (1σ, $n = 58$) ppm, agreeing well with the certified value of 5.43 ± 0.14 (1σ) ppm. Repeated analysis of the United States Geological Survey rock reference material AGV-1 resulted in U concentration of 1.900 ± 0.049 (1σ, $n = 3$) ppm, also in agreement with the literature value of 1.903 ± 0.010 ppm (Jochum et al., 2016). Repeated analysis of an in-house marine sediment standard yielded long-term (over 3 years) reproducibility (1 relative standard deviation [SD], $n = 57$) of ~4% of measured values for Mo and of ~6% of measured values for U.

We report Mo and U as Element/Aluminum (Al) ratios to distinguish authigenic accumulation from the terrigenous background (Cartapanis et al., 2011; J. Muratli et al., 2010). Al was analyzed using an inductively coupled plasma optical emission spectrometer (ICP-OES) at the same lab. Repeated analysis of the sediment reference material PACS-2 gave an Al concentration of 6.45 ± 0.16 (1σ, $n = 58$) wt% consistent with the certified value of 6.62 ± 0.16 (1σ) wt%. Procedural blanks of Al were negligible (<0.1%). Long-term (over 3 years) reproducibility (1 relative SD, $n = 57$) of Al were ~2%. The choice of terrigenous normalization is however not essential given that Al and Ti, two most widely used elements for terrigenous background, at both sites varied little (<5%) during the entire record, suggesting that the variabilities of Mo and U concentrations were dominated by authigenic accumulation.

2.3. Correspondence Between Faunal Changes and Redox-Sensitive Metals

We obtained redox sensitive metal concentrations and benthic foraminiferal faunal counts from the same samples, making it possible to quantitatively compare the two types of data. In total, we have 355 samples with both faunal and redox metals data (Table S1). We use the Mantel correlation to test the hypothesis that samples that are most dissimilar in faunal composition are also most dissimilar in their concentrations of redox metals. For these analyses, we calculated Bray-Curtis dissimilarity among samples using the proportional abundances of species and the Euclidean dissimilarity among samples using the z-score transformed redox metals data (Mo/Al, U/Al); the Euclidean dissimilarity metric accommodates negative values unlike the Bray-Curtis dissimilarity, which is most appropriate for faunal abundances (McCune et al., 2002). Z-score transformations were performed using the *scale* function of the "base" package in R (R Core Team, 2016).

Each redox sensitive metal has different threshold sensitivity to changes in oxygenation and, thus, may have a different relationship to the faunal gradients. To test if Mo/Al and U/Al differ in the strength of their correlation to the primary axis of faunal variation, we calculate the Spearman correlation between faunal DCA Axis 1 scores and individual redox-sensitive metal concentrations. All correlations were also performed for

each size fraction separately to test the hypotheses that faunal variation is similarly associated with differences in redox metals concentrations regardless of the size fraction.

2.4. Quantifying Dissolved Oxygen Concentrations From Faunal Assemblages

Further, we quantitatively estimate oxygenation values from benthic foraminiferal faunal assemblages using the Behl dissolved oxygen (BDO) index following K. Ohkushi et al. (2013). However, in its original implementation, this index was restricted to the 19 species for which the authors acquired oxygen tolerances reported in the literature (K. Ohkushi et al., 2013). Of these 19 species, we found 14 in our samples and used these species to calculate a "literature-based" BDO estimate comparable to this previous work (Table S2). In order to instead use all species in our analyses, we also calculate a modified BDO using the covariation of species with known oxygenation tolerances in DCA ordination spaces to place unassigned species into dysoxic (>1.83 DCA species scores), suboxic (−0.39 to 1.83), or weakly hypoxic to oxic (<−0.4) categories (see Section 3.3). To assess whether the faunal size fraction examined can affect these calculated oxygenation values, we compare BDO results using the >63 μm size fraction and the >125 μm size fraction.

2.5. Comparing Fossil Assemblages to Modern Surface Sediment Assemblages

We further compare our fossil assemblages (>63 μm size fraction) to 225 benthic foraminifera assemblages collected from sediment surface samples following Belanger et al. (2016) to identify fossil assemblages indicative of oxygenation values outside the range of modern spatial variability in GoA. Samples were compiled from Bergen and O'Neil (1979), Echols and Armentrout (1980) and from EW0408 and IODP Expedition 341 coretops (Belanger et al., 2016). The data set includes at least 13 samples from within the modern OMZ. As in previous work, we consider a fossil sample to have no modern analog if its nearest-neighbor Spearman rho coefficient is less than 0.1285, which we calculated from the 95th percentile of the dissimilarity among modern-modern sample pairs (Belanger et al., 2016). We use Spearman rho because it considers only the rank abundance of taxa and, thus, minimizes the dissimilarity due to differences in the proportional abundances of species. Fossil assemblages for which we identify analogs are also assigned to a primary environment (i.e., slope or shelf) based upon the environment of their nearest modern analog.

Modern species represented in the fossil data set were assigned to the same oxygen categories as in the fossil calculations. The 27 modern species not found in the fossil data set were assigned to oxygen categories based upon the correlation between their relative abundances in a modern sample and the modern oxygen values of the collection site estimated from the World Ocean Atlas (WOA) 2013 (Garcia et al. 2013). Species with a positive correlation with oxygen concentrations were assigned to the oxic category and species with a negative correlation to the suboxic category (Table S3). Samples with flagged WOA data for oxygenation were excluded from analyses requiring oxygen concentrations leaving 208 modern samples with modern oxygen measurements.

2.6. Identifying the Occurrence, Severity, and Duration of Hypoxic Events

To quantitatively distinguish low-oxygen events from background conditions, we extract the most extreme values for each oxygenation proxy (DCA Axis 1 score, Mo/Al, and U/Al) in our time series using the 95th, 95–90th, and 80–90th upper quantiles where the 95th upper quantile represents data in the highest 5% of values. We focus on the change in DCA Axis 1 because this Axis summarizes the majority of our faunal variation and is well related to oxygenation (see Section 3.1). This method ensures that all proxies yield the same number of potential low-oxygen events. Further, we used the BDO values calculated from >63 μm data set to operationally categorize the events into dysoxic (<0.5 ml/L), suboxic (0.5–1 ml/L), and weakly hypoxic to oxic (>1 ml/L) conditions. Because we are primarily interested in identifying low-oxygen events and the BDO index is known to underestimate oxygenation at higher values, we conservatively define the threshold between suboxic and weakly hypoxic to oxic conditions at 1 ml/L instead of the 1.4 ml/L used by others (Moffitt et al., 2015; K. Ohkushi et al., 2013). Using these data, we can then ask whether proxies agree or disagree on the presence, duration, and relative severity of a low-oxygen event.

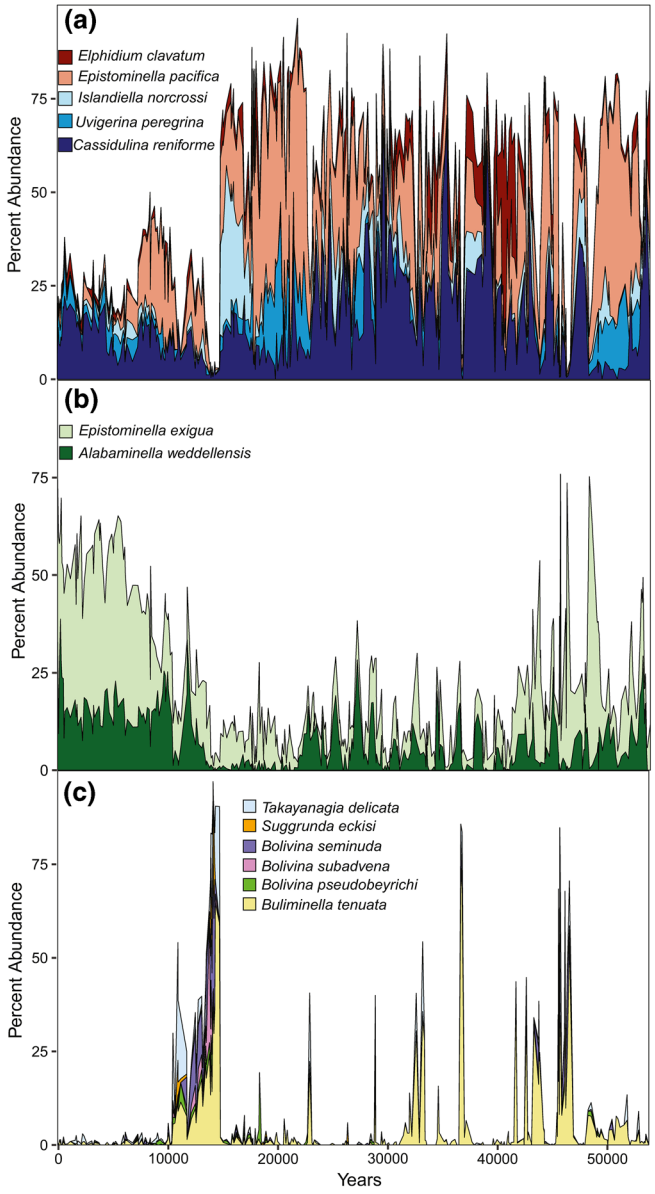

Figure 2. Relative abundance of numerically and ecologically significant benthic foraminiferal species in the >63 μm size fraction. (a) Five of the most frequently occurring species that are also have high abundances in the glacial. (b) Opportunistic species. (c) Six species with reported oxygen tolerances <0.1 ml/L.

2.7. Rates of Faunal and Environmental Change

DCA axes are scaled in units of SDs of total faunal variation (McCune et al., 2002), thus we can use DCA Axis 1 scores to quantify rates of ecological change as in other paleoecological studies (Correa-Metrio et al., 2012). We also calculate the rate of change in oxygenation using our modified BDO values. We recalculate the rate of BDO change after removing shelf analogs to provide a more conservative rate estimate that accounts for potential downslope transport and faunal changes due to major sedimentation changes.

3. Results

In total, we identified 74 species and congeneric groups of benthic foraminifera in the >63 μm size fraction. Of the 74 species, 26 comprised less than 2% of any one sample and, thus, were removed from the analyses leaving 48 species. From the full faunal list, 67 species occur in the 63–125 μm size fraction and 67 species occur in the >125 μm size fraction (Table 1). The most frequently observed species regardless of size fraction are *Cassidulina reniforme, Epistominella pacifica, Uvigerina peregrina, Islandiella norcrossi, Elphidium clavatum, Alabaminella wedellensis,* and *Epistominella exigua* and together they often comprise the majority the assemblage in the >63 μm size fraction (Figures 2a and 2b). Only 9% of the taxa present in the >63 μm size fraction are absent from the >125 μm size fraction. Some species, including *Bolivina earlandi, Loxostomum minuta, Bolivina decussata, A. wedellensis,* and *E. exigua,* are abundant in the 63–125 μm size fraction and are rare to absent in the >125 μm fraction (Table S1). For example, *A. wedellensis* and *E. exigua,* which are used as proxies of organic carbon fluxes (Gooday, 1993; Gooday & Jorissen, 2012; Sun et al., 2006), comprised up to 76% of the assemblage in the 63–125 μm size fraction but are less than 6% of the assemblage in the >125 μm size fraction (Figure S1).

3.1. Primary Gradients in Faunal Composition

DCA Axis 1 summarizes 51%–55% of the faunal variation whereas DCA Axis 2 summarizes 6%–19% of the faunal variation depending on the size fraction analyzed (Table 1). The position of samples in the total DCA space (Axes 1–4) has a strong positive Mantel correlation among all three size-fractions; sample position along DCA Axis 1 alone is also similar among size fractions (Table 2). Species positions in total DCA space are also positively correlated among size fractions, but with weaker associations among size fractions than for site positions in DCA space (Table 2). Given these similarities among the ordinations and their temporal patterns regardless of size fraction (Figure 3; Table S4), we will only discuss the DCA results using the >63 μm data set.

Species with the most positive DCA Axis 1 scores include *Buliminella tenuata*, *Takayanagia delicata, Bolivina seminuda, Bolivina subadvena, Bolivina pseudobeyrichi,* and *Suggrunda eckisi* (Figure 4; Table S5); these taxa are common in dysoxic to suboxic settings (Erdem & Schönfeld, 2017; K. Ohkushi et al., 2013; Schmiedl et al., 2003; Tetard et al., 2017) and sometimes dominate our assemblages (Figure 2c). Species with strong negative DCA Axis 1 scores include *I. norcrossi, Stainforthia complanata*, *Astrononion gallowayi, Nonionella digitata, Triloculina trihedra, E. clavatum, Quinqueloculina* spp., *Virgulina* spp., *Stainforthia fusiformis*, a phytodetritus-feeding opportunist related to ephemerally low-oxygen environments (Alve, 2003), has a low negative DCA Axis 1 score. Other opportunistic species sensitive to the seasonality of productivity and flux

Table 2
Pairwise Mantel Correlations Between DCA Site Scores for the Three Benthic Foraminiferal Size Fractions (>63 μm, >125 μm, and 63–125 μm)

DCA score comparison	>63 μm and >125 μm	>63 μm and 63–125 μm	>125 μm and 63–125 μm
DCA Axes 1–4 sample scores	0.82 (0.81–0.83)**	0.80 (0.79–0.80)**	0.58 (0.57–0.60)**
DCA Axis 1 sample scores	0.82 (0.81–0.82)**	0.93 (0.93–0.94)**	0.76 (0.75–0.77)**
DCA Axes 1–4 species scores	0.28 (0.24–0.33)*	0.50 (0.47–0.55)**	0.18 (0.14–0.22)*
DCA Axes 1 species scores	0.65 (0.62–0.70)**	0.83 (0.82–0.85)**	0.47 (0.43–0.53)**

Note. Mantel *r*-values are reported with 95% confidence intervals for each correlation in parentheses.
*$p < 0.05$; **$p < 0.01$.

of fresh phytodetritus, including *A. wedellensis* and *E. exigua* (Gooday, 1993; Gooday & Jorissen, 2012; Sun et al., 2006), have low positive (*A. wedellensis*) and high positive (*E. exigua*) DCA Axis 1 scores and dominate assemblages in the Holocene interval of our record (Figure 2b). Species associated with glacial conditions, including *E. pacifica* and *C. reniforme* (K. I. Ohkushi et al., 2003), and oxic settings, such as *Pyrgo* spp. and *Quinqueloculina* spp. (K. Ohkushi et al., 2013), have negative DCA 1 Axis scores. *Nonionellina labradorica*, categorized by others as a taxon that favors oxic environments (K. Ohkushi et al., 2013), has a low positive DCA Axis 1 score in our analyses.

Species with positive DCA Axis 2 scores include phytodetritus sensitive taxa such as *N. labradorica, S. fusiformis, A. wedellensis*, and *E. exigua* (Cedhagen, 1991; Sun et al., 2006); these species are dominant in some samples with DCA Axis 2 scores >0.5 (Figure 4; Table S5). Other species with positive DCA Axis 2 scores include *Bolivina decussata, Trifarina angulosa, B. subadvena*, *T. trihedra, Nonion grateloupii, Valvulineria* spp., *C. reniforme*, *and Cassidulina* spp. Some low-oxygen tolerant taxa, including *B. seminuda* and *S. eckisi*,

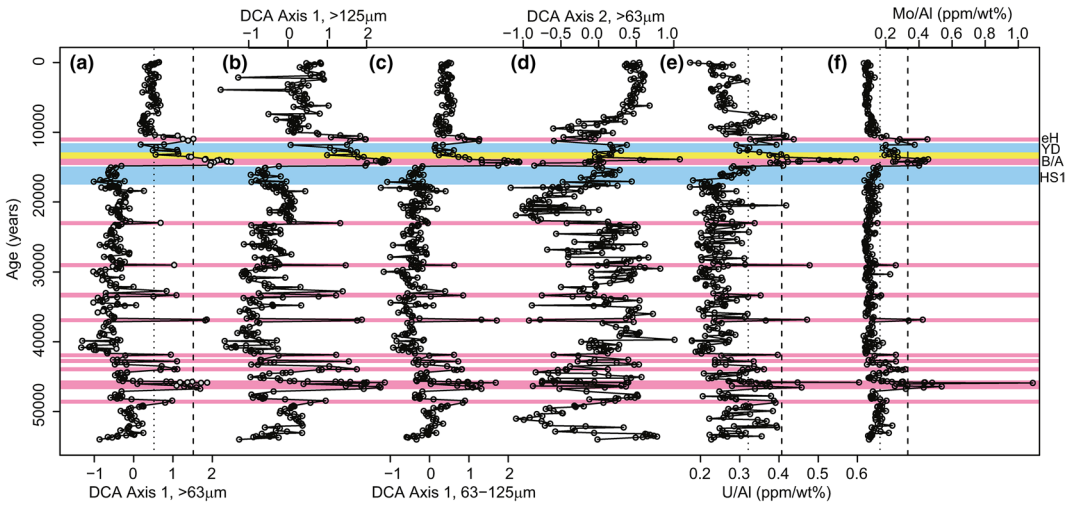

Figure 3. Ecological and environmental proxies for Site U1419 in the Gulf of Alaska for the last 54 ka. (a–c) Detrended Correspondence Analysis (DCA) Axis 1 scores of benthic foraminiferal assemblages using each of three size fractions (>63 μm, >125 μm, and 63–125 μm). In (a), assemblages with no modern analog are indicated with gray-filled symbols. (d), DCA Axis 2 scores for the >63 μm size fraction. Redox metal values from the same samples: (e), U/Al, (f), Mo/Al. Vertical dashed line in (a), (e), and (f) represents the upper 95th upper quantile and the dotted line represents upper 80th upper quantile of the data distribution. Climate intervals indicated as eH, early Holocene; YD, Younger Dryas; B/A, Bølling-Allerød; and HS1, Heinrich Stadial 1. Pink bars represent dysoxic events discussed in the text, blue bars are oxic intervals discussed in the text. The Allerød is distinguished from the Bølling in yellow.

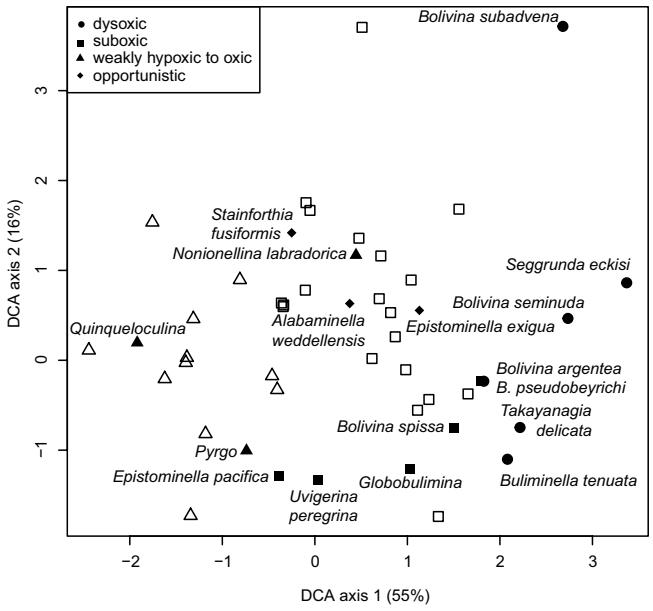

Figure 4. Detrended correspondence analysis (DCA) species scores for benthic foraminiferal assemblages from the >63 μm size fraction. Circles indicate species with a lowermost oxygen tolerance below 0.1 ml/L O_2, squares indicate species with a lowermost oxygen tolerance of 0.1–0.5 ml/L O_2, and triangles indicate those with a lowermost oxygen tolerance above 0.5 ml/L O_2 based upon published tolerances (Table S2). Diamonds denote opportunistic taxa, which are also inferred to tolerate suboxic conditions. Filled symbols indicate species for which environmental preferences were obtained from the literature and are labeled with species names. Open symbols denote species assigned to a category based on its DCA Axis 1 score.

have positive DCA Axis 2 scores; however, other low-oxygen tolerant taxa including *T. delicata*, *B. tenuata*, and *B. pseudobeyrichi* have negative DCA Axis 2 scores.

3.2. Correspondence Between Faunal and Redox Metal Variation

Samples that are most dissimilar in their faunal composition are also most dissimilar in their redox metal concentrations in all three size-fractions we tested (Mantel correlations, Table 1). Individual redox-sensitive metal concentrations (Mo/Al and U/Al) and the primary gradient of faunal composition (DCA Axis 1 scores) also positively covary regardless of size fraction (Table 1), such that samples with higher DCA Axis 1 scores have higher redox metal concentrations. This is consistent with the positive DCA Axis 1 scores of low-oxygen tolerant species. U/Al has a stronger positive correlation (Spearman's rho = 0.61) with DCA Axis 1 scores as compared to Mo/Al (Spearman's rho = 0.45). In contrast to DCA Axis 1, DCA Axis 2 has weaker correlations with redox metal concentrations and no systematic relationship with low-oxygen tolerant species (Table 1; Figure 4).

3.3. Quantifying Oxygenation From Faunal Assemblages

Published oxygen tolerances indicate six species associated with dysoxic conditions (lowermost oxygen tolerances <0.1 ml/L O_2) and five species associated with suboxic conditions (lowermost oxygen tolerances 0.1–0.5 mL/L O_2) are present in our data set (Table S2). Following previous studies using similar methods (K. Ohkushi et al., 2013; Tetard et al., 2017), only three "weakly hypoxic to oxic" species (*N. labradorica*, *Pyrgo* spp., and *Quinqueloculina* spp.) are used in our "literature-based" BDO calculations. Using this subset of 14 species produces BDO values between 0.10 and 1.25 ml/L (Figure 5a, Table S4).

All species designated as dysoxic in the literature have DCA Axis 1 scores greater than or equal to 1.83. Species categorized as suboxic indicators in the literature have with DCA Axis 1 scores between −0.39 and 1.83, thus we assign species without literature-based oxygen tolerances that fall within this range of DCA Axis 1 scores to the suboxic category. We categorize all species without published oxygen tolerances with DCA Axis 1 scores less than -0.4 as weakly hypoxic to oxic, consistent with the DCA Axis 1 scores of *Pyrgo* spp., and *Quinqueloculina* spp. (Figure 4, Table S3). Oxygen values calculated using the >63 μm data set produce values between 0.12 and 1.40 ml/L O_2; restricting to foraminifera >125 μm produces values from 0.11 to 1.50 ml/L O_2 (Figures 5b and 5c).

On average, BDO calculations using only those species with published oxygen tolerances reconstruct oxygen values 0.30 ml/L O_2 (IQR = 0.15–0.43) lower than calculations using all species in the >63 μm size fraction (Figure 6). Oxygen estimates from the literature-based calculations tend to frequently produce values of ~0.5 ml/L O_2 whereas calculations for these same samples are 0.5–1.2 ml/L O_2 using the total fauna. In contrast, oxygen calculations using the >125 μm size fraction are similar on average to the >63 μm size fraction (median difference = 0.05 ml/L, IQR = −0.04 to 0.10; Figure 6).

3.4. Oxygen Estimates From Modern Faunas

Core top assemblages from Site U1419 and EW0408-84MC have an average BDO estimate of 0.60 ml/L O_2 using the full fauna (>63 μm size fraction), similar to the 0.59 ml/L O_2 estimates for the modern site derived from the WOA (Table S6). Oxygen calculations from our modified BDO index and the modern measured oxygen concentrations have a strong positive correlation (Spearman rho = 0.81, p <<0.001), but the values are different in scale (Figure 6c). The calculated oxygen estimates are higher than measured values when

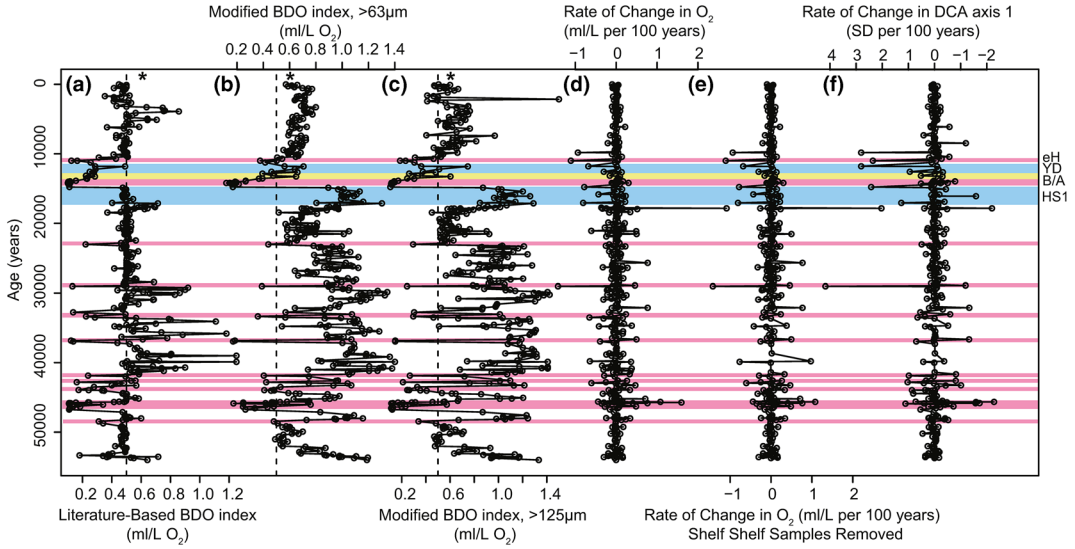

Figure 5. Rates of oxygenation and ecological change. (a) Dissolved oxygen values calculated using the Behl dissolved oxygen (BDO) index and only species whose oxygen tolerances are known from the literature. (b) Dissolved oxygen values calculated using the total assemblage and (c) using the >125 μm size fraction. (d) Rate of oxygenation change per 100 years using all samples. (e) Rate of change in oxygenation per 100 years with shelf analogs removed. (f) Rate of change in detrended correspondence analysis (DCA) Axis 1 scores per 100 years using all samples. All metrics are derived from the >63 μm size fraction unless otherwise specified. Dashed lines in a–c indicate 0.5 ml/L are dysoxic-suboxic O_2 threshold. Climate intervals indicated as eH, early Holocene; YD, Younger Dryas; B/A, Bølling-Allerød; and HS1, Heinrich Stadial 1. Pink bars represent low oxygen events discussed in the text, blue bars are the oxic events. Allerød is distinguished from the Bølling in yellow.

WOA values are <0.5 ml/L (median difference = 0.26 ml/L, IQR = 0.15–0.39), similar for WOA values 0.5–1.5 ml/L (median difference = −0.09 ml/L, IQR = −0.17 to 0.09) and lower than measured values when WOA values are >1.5 ml/L (median difference = −5.29 ml/L, IQR = −5.49 to −4.34).

3.5. Defining the Occurrence and Duration of Low-Oxygen Events

Of the 355 samples we analyzed, 129 have at least one low-oxygen proxy (DCA Axis 1 score, U/Al or Mo/Al) that exceeds the 80th upper quantile of the data for that variable (Figure 3). In total, we found 71 samples in which all the proxies suggest low-oxygen conditions. For the majority of the record, all three faunal size fractions indicate similar DCA Axis 1 excursions with minor differences in the relative severity (Figure 3). During the mid-Holocene (~6.8 ka) to present, many samples have DCA Axis 1 scores in the upper 80–90th quantile, but these samples do not have correspondingly high redox metal concentrations (Figure 3). Similarly, some Holocene samples from 8.5 to 7.4 ka and MIS 3 samples from 53.5 to 49.2 ka have redox metal concentrations in the 80th upper quantile without corroborating DCA Axis 1 scores. However, these are exceptions and the majority of samples that have high positive DCA Axis 1 scores have high redox metal concentrations.

High DCA Axis 1 scores and high concentrations of redox metals also generally correspond to low BDO estimates. All samples with either DCA Axis 1 scores or redox metals concentration in the 80th upper quantile have BDO values suggesting dysoxic or suboxic conditions. Most of the severe dysoxic events with <0.5 ml/L BDO estimates contain fewer than 5% oxic species. Mo/Al values in the 95th upper quantile correspond to median BDO values of 0.23 ml/L (IQR = 0.18–0.40), significantly lower than DO estimates of 0.41 ml/L for samples with Mo/Al values in the 90–95th upper quantile (Mann-Whitney $U = 258$, $p = 0.0013$; Table 3). Similarly, Mo/Al values in the 90–95th upper quantile have BDO estimates that are significantly lower than the median BDO estimates of 0.59 ml/L in the 80–90th upper quantile ($U = 1{,}188$, $p < 0.0001$, Table 3). Increasing U/Al values also correspond with increasing faunal DO estimates. The BDO estimates in samples with U/Al in for the >95th upper quantile (Mann-Whitney $U = 76$, $p = 0.0034$) are significantly lower than for samples in than 90–95th U/Al quantile (Mann-Whitney $U = 244$, $p = 0.0049$) and 80–90th quantile (Mann-Whitney $U = 1{,}079$, $p < 0.0001$; Table 3).

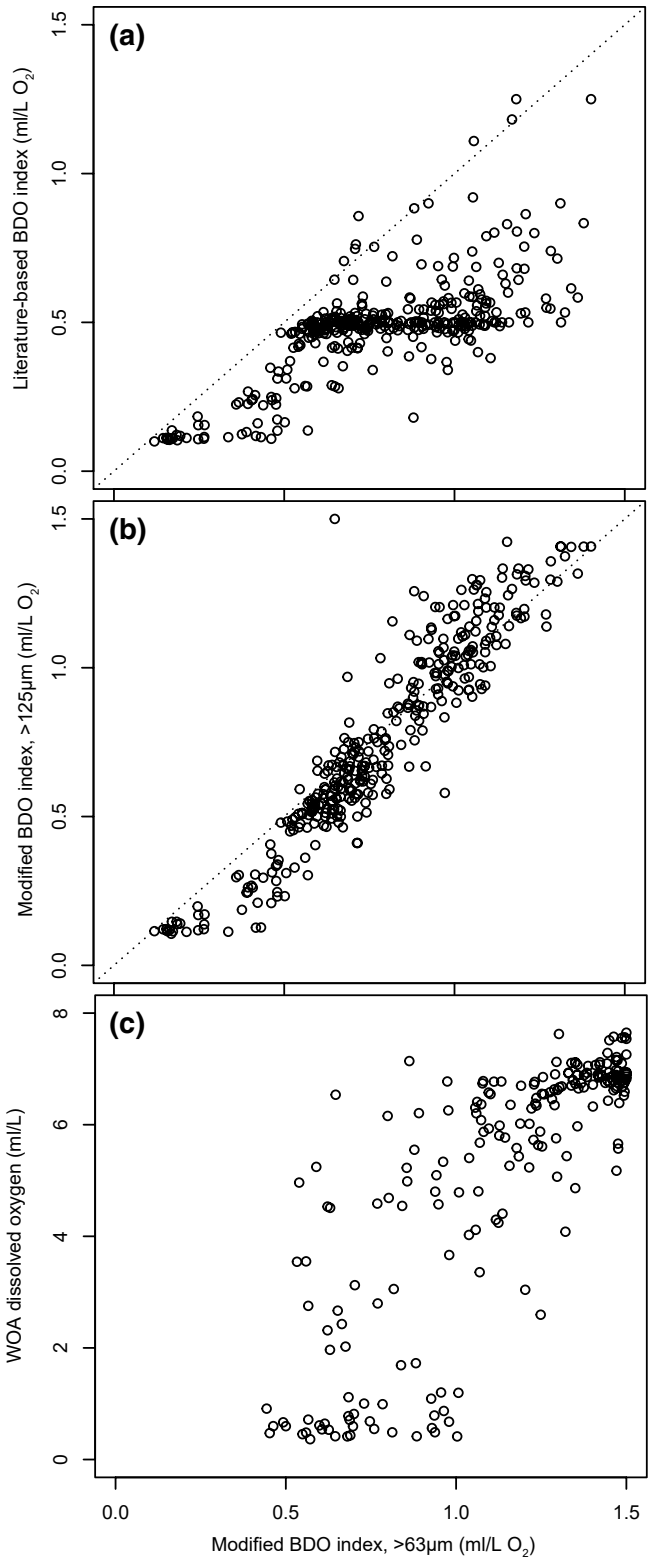

Figure 6. Relationships among dissolved oxygen calculations for (a) fossil assemblages using only 14 species with published oxygen tolerances and fossil assemblages using all 48 species in the >63 μm size fraction, (b) fossil assemblages from the >63 μm size fraction and fossil assemblages from the >125 μm size fraction, and (c) modern assemblages in the >63 μm size fraction and measured dissolved oxygen values from the World Ocean Atlas 2013 (Garcia et al., 2013). In (a and b), BDO values are the same as in Figures 5a–5c and dotted lines are 1:1 lines.

Table 3
Upper Quantile Values for Faunal and Geochemical Oxygenation Proxies

	Proxy value range	Median faunal >63 dissolved oxygen estimate (ml/L)
Mo/Al (ppm/wt%)		
95th upper quantile	0.34–1.09	0.23 (0.18–0.40)
90–95th upper quantile	0.25–0.33	0.41 (0.37–0.46)
80–90th upper quantile	0.16–0.25	0.59 (0.50–0.68)
U/Al (ppm/wt%)		
95th upper quantile	0.41–0.60	0.30 (0.18–0.45)
90–95th upper quantile	0.37–0.41	0.49 (0.40–0.63)
80–90th upper quantile	0.32–0.37	0.55 (0.43–0.68)
DCA Axis 1 (sample scores)		
95th upper quantile	1.52–2.50	0.19 (0.16–0.26)
90–95th upper quantile	1.05–1.51	0.42 (0.39–0.47)
80–90th upper quantile	0.52–1.05	0.60 (0.52–0.64)
75–80th upper quantile	0.44–0.52	0.68 (0.64–0.71)

Note. Faunal dissolved oxygen estimates are from the BDO index using the full fauna in the >63 μm size fraction. Interquartile ranges on the medians are in parentheses.

The lowest BDO estimates occur during the B/A and during discrete intervals in MIS 3 as indicated by both the faunal and redox sensitive metals. DCA Axis 1 scores (>63 μm data set) exceeding the 95th and 90th upper quantile of the faunal data occur in samples from the Bølling (14.7–13.8 ka) and the Allerød (13.8–12.9 ka), respectively (Table 3). The B/A interval had the lowest calculated DO values (0.12 ml/L from modified BDO >63 μm) in the ~54 ka record with a median value = 0.20 ml/L; IQR = 0.16–0.37. The B/A is also corroborated by redox metal values in the 80th upper quantile. Within the B/A, the Bølling had lower BDO values (0.12–0.26 ml/L) and most samples have redox values in the 95th upper quantile. In the Allerød, however, BDO estimates were greater than 0.26 ml/L and redox values where in the 80-90th upper quantile (Figures 3 and 5). DCA Axis 1 scores and redox metal concentrations are also in the upper 90th quantile from 46.7 to 45.7 ka with median BDO estimates of 0.42 ml/L (IQR = 0.25–0.46 ml/L; Figures 3 and 5).

In addition to the excursions in the B/A and MIS 3 discussed above, shorter duration excursions occur during MIS 3. DCA scores >1.52 occur in two adjacent samples at ~36.9 ka with BDO value of 0.18 ml/L and are corroborated by Mo/Al values in the 95th upper quantile and U/Al values in the upper 80th quantile. BDO estimates as low as 0.38 ml/L occur from 11.2 to 10.9 ka during the early Holocene and are associated with DCA Axis 1 scores in the upper 90th quantile and redox metal values in the upper 80th quantile. Faunal assemblages and both redox sensitive metals also have values in the upper 80th quantiles in single samples at 23, 29, 33.3, 41.8, and 42.8 ka and in a sample pair at ~48.5 ka. These shorter (<150 years) events have BDO values ranging from 0.36 to 0.44 ml/L. In addition, five consecutive samples from 44–43.5 ka have scores in the 80–95th upper quantile with BDO values ranging from 0.40 to 0.53 ml/L (Figure 5). All of these shorter MIS 3 events are corroborated by Mo/Al and U/Al values in the upper 80th quantile with the exception of the 23 ka event where U/Al is not in the upper 80th quantile.

When proxy values are less extreme, correspondence becomes less common. For example, DCA Axis 1 scores in the 80–95th upper quantile (scores 0.52–1.51) occur immediately following the B/A event between 13.6 and 11.7 ka, similar in timing to the Younger Dryas (YD; 12.9–11.7 ka). These YD samples also have Mo/Al values in the upper 80th quantile, however only two of five samples have U/Al values in the upper 80th quantile. In the younger record from ~7 ka to present, DCA Axis 1 scores are in the 75–90th upper quantile with the median BDO values of 0.68 ml/L (IQR = 0.64–0.72 ml/L), but both redox sensitive metals have values below the 80th quantile for the entire interval. Further, during MIS 3, samples from ~53 to 48 ka have redox metals values in the upper 80th quantiles, however, with the exception of two samples, DCA Axis 1 scores are below the upper 80th quantile (median BDO = 0.72 ml/L; IQR = 0.58–0.98 ml/L).

3.6. Rates of Faunal and Environmental Change

Changes in faunal composition along DCA Axis 1 are minor between sequential samples with a median absolute ecological change between samples of 0.11 SDs per 100 years (IQR = −0.11 to 0.12). Changes in DCA Axis 1 sample scores exceeding 1 SD/100 years toward higher scores occur 11 times in the record and 12 times toward lower scores; changes exceeding 2 SD/100 years occur five times toward higher DCA Axis 1 scores and thrice toward lower scores (Figure 5). The most rapid faunal shift toward higher DCA Axis 1 scores occurs at 29 ka with additional changes >2 SD/100 years at 9.8, 11.0, 11.8, and 14.8 ka. Similarly, changes in oxygenation values calculated using the modified BDO index (>63 μm size fraction) are generally low between adjacent samples with a median absolute change of 0.07 (IQR = 0.03–0.17) ml/L per 100 years. However, changes in oxygenation exceeding 0.5 ml/L per 100 years occurs 18 times and changes exceeding 1 ml/L per 100 years occurs five times in our record (Figure 5). Of these, 10 are decreases in

oxygenation and 8 are increases in oxygenation. The most rapid oxygenation changes co-occur with rapid changes in DCA Axis 1 scores (Figure 5).

Of the 355 fossil assemblages, 50 are most similar to samples from the modern shelf (Table S7). Thus, we reevaluated changes in oxygenation after removing all the samples that are most similar to the shelf samples to reduce the potential influence of downslope transport on the abruptness of faunal changes. All retained fossil samples had modern analogs from water depths greater than 473 m. Some abrupt changes in DCA Axis 1 scores are diminished as faunal shifts are now stretched over greater potential time or are offset to occur earlier (Figure 5). In this restricted set of calculations, the median absolute change in oxygenation is 0.06 (IQR = 0.02–0.16) ml/L per 100 years. Changes in oxygenation exceeding 0.5 ml/L per 100 years occur 15 times and changes exceeding 1 ml/L per 100 years occur four times (Figure 5).

4. Discussion

4.1. Primary Determinant of Faunal Composition is Oxygenation

Benthic foraminifera are commonly used as marine paleo-oxygenation proxies, however confounding environmental factors such as organic carbon availability can complicate their use (Gooday, 1993; Gooday & Jorissen, 2012; Jorissen et al., 2007). In our approach to reconstructing the oxygenation history of GoA, we first use multivariate analyses of species-level faunal assemblages to detect faunal gradients and cross-validate the gradients using concentrations of redox-sensitive metals measured on the same sediments from which we collected the foraminifera. We find that the redox-sensitive metal concentrations generally increase with increasing DCA Axis 1 scores, suggesting that, while these co-registered proxies are independently measured, they reflect a similar oxygenation gradient. This interpretation is further supported by high positive DCA Axis 1 scores for species associated with dysoxic conditions in modern environments. The stronger association between DCA Axis 1 and U/Al than between DCA Axis 1 and Mo/Al suggests that benthic foraminiferal assemblage composition is sensitive to oxygen variation at suboxic levels and is not simply responding to a threshold condition such as the presence or absence of sulfidic conditions.

The positive association between redox sensitive metal concentrations and the position of samples in the overall faunal ordination space further underscores the importance of oxygen in structuring the GoA assemblages. Species known to respond positively to phytodetritus input have the most influence on DCA Axis 2 scores, suggesting that this secondary, orthogonal, axis reflects differences in organic carbon availability. Unlike DCA Axis 1, species with known tolerances for low-oxygen conditions have both positive and negative DCA Axis 2 scores, suggesting little direct influence of oxygenation on DCA Axis 2. Our previous analysis of benthic foraminiferal faunas at two sites in GoA extending to ~23 ka also found that variation in oxygen-sensitive and productivity-sensitive components of the fauna were separated on different ordination axes (Belanger et al., 2020). The separation of oxygen-sensitive and productivity-sensitive components of the faunal variation in our GoA records on orthogonal axes strengthens our ability to use DCA Axis 1 scores as the basis for estimating quantitative oxygenation changes.

4.2. Sensitivity of Faunal and Environmental Gradients to Size Fraction

Inconsistencies in the faunal size fraction examined among studies can pose a challenge for comparisons among regions and could inadvertently bias the reconstructed oxygenation histories (Schönfeld et al., 2012; Weinkauf & Milker, 2018). While some studies suggest using only individuals >125 μm is more efficient and does not strongly affect environmental or ecological interpretations (Bouchet et al., 2012; Schönfeld et al., 2012), the smaller size fractions (63–125 μm) may contribute important faunal variation in eutrophic or low-oxygen settings (Gooday & Goineau, 2019; Schönfeld et al., 2012). In addition, comparisons of the >125 μm and >150 μm size fractions show that subtle variations between size fractions can contribute significant variations in assemblage counts and subsequent multivariate analyses (Weinkauf & Milker, 2018).

Comparisons among analyses using different size fractions herein, however, suggest that faunal variation is similarly captured regardless of size fraction (Figure 3). While the majority of foraminiferal individuals are in the 63–125 μm size fraction in the GoA data set, the taxonomic composition is similar among size fractions. Further, faunal variation is partitioned similarly among DCA axes in each size fraction and the

position of samples in DCA space is similar between the analyses. However, the position of species in DCA space is not as well correlated among size fractions, suggesting that species positions in ordination space are not as stable as sample positions, which incorporate the relative abundances of all species. Together, these comparisons suggest that analyses using total faunas are likely to replicate similar ecological and environmental gradients regardless of size fraction, but size-fraction choices may affect analyses that rely on index taxa.

4.3. Quantifying Paleo-Oxygenation in the GoA

Differences in the taxa incorporated into oxygen reconstructions could also affect the perceived severity of low-oxygen events in paleoceanographic records, however index taxon methods prevail in the literature, even among studies incorporating multivariate faunal analyses (e.g., K. Ohkushi et al., 2013; Tetard et al., 2017). For the GoA, BDO calculations restricted to literature-derived oxygen tolerances reconstruct significantly lower oxygen concentrations than the full fauna; the disproportionate inclusion of species at the low-oxygen end of the faunal gradient in the literature-based calculations likely drives this bias (Figure 6a). In contrast, there is no systematic difference between oxygenation values calculated using all taxa in the >63 μm size fraction compared to all taxa in the >125 μm size fraction (Figure 6b). Thus, taxonomic inclusion affects these oxygen calculations, but, when using all observed species, size fraction choices introduce no systematic bias for the GoA record Figure 6.

For the GoA site, our modified BDO index accurately reconstructs the modern measured oxygen concentrations using the full fauna from modern surface sediment samples, suggesting our assignment of taxa to oxygenation categories reflects the foraminiferal tolerances well. Further, the dissolved oxygen calculations for the modern assemblages are positively related to the modern measured oxygen values suggesting that the faunas successfully record relative differences in oxygenation. However, the BDO values severely underestimate oxygen concentrations above 1.5 ml/L (Figure 6c). This limitation is expected given the equation is restricted to producing values between 0.1 and 1.5 ml/L. Further, foraminiferal assemblages do not tend to vary in response to oxygenation above >1 or 2 ml/L (Moffitt et al., 2015; Murray, 2001), but modern oxygen concentrations in the data set exceed 7 ml/L. K. Ohkushi et al. (2013) further suggested that the BDO index overestimates the lowest oxygen values. This is reflected in GoA in the overestimate of modern oxygenation for sites with WOA oxygen concentrations <0.5 ml/L (Figure 6c). Differences between the measured dissolved oxygen and the BDO values may also occur because the WOA values are from near-bottom waters rather than at the sediment-water interface or within pore waters where benthic foraminifera reside. Our modified BDO index is not systematically biased for modern oxygen concentrations between 0.5 and 1.5 ml/L and, thus, may be most reliable for observed oxygen values in that range. Despite these potential inaccuracies, calculated BDO values <45 ml/L occur when Mo/Al values are in the 90th upper quantile of our data set, consistent with measurable Mo accumulation occurring at O_2 values <0.51 ml/L (Zheng et al., 2000). Further, samples with the highest Mo/Al values (upper 95th quantile of our data) have a median BDO value of 0.23 ml/L, consistent with the interpretation that the presence of authigenic Mo suggests bottom water oxygen values <0.22 ml/L (Zheng et al., 2000). Mo/Al values as low as 0.25 ppm/wt% also straddle the dysoxic-suboxic boundary reconstructed by the faunal assemblages while lower Mo/Al values correspond to the more oxic faunas. Thus, the oxygenation values reconstructed by the faunas are consistent with the known redox behavior of Mo. Similarly, higher U/Al values correspond tend to correspond with lower BDO estimates from the faunas.

Given the faunal-based BDO calculations herein tend to overestimate oxygenation at the lowest values, and low BDO estimates are strongly associated with the highest Mo/Al values, we are confident that when the calculation produces oxygen concentrations <0.5 ml/L, the conditions were indeed dysoxic. Using these methods, we find either 21 or 32 fossil samples that indicate lower oxygen conditions in the past 54 ka than present in the modern GoA data set based upon WOA-derived data (minimum of 0.36 ml/L O_2) or the BDO estimates using modern benthic foraminiferal assemblages (minimum of 0.44 ml/L O_2), respectively. This suggests that this upper OMZ site experienced lower oxygen conditions in the past than anywhere in the modern GoA. While benthic foraminiferal proxies primarily reflect pore water oxygenation, previous studies have related low (<5%) abundances of oxic taxa to I/Ca values from epifaunal benthic foraminifera that suggest dysoxic bottom waters (Taylor et al., 2017). In our record, species assigned to the weakly-hypoxic

to oxic category make up fewer than 5% of individuals in samples with the lowest BDO values. Thus, when our benthic foraminiferal faunas indicate extreme dysoxia in the pore waters, oxygen was likely also low in the bottom waters.

The environmental tolerances of benthic foraminifera most abundant in our lowest oxygen samples also support past low-oxygen conditions with no modern analog in the GoA. Species that dominate our lowest oxygen assemblages, such as *B. tenuata*, *B. seminuda, and B. argentea,* are rare in the modern GoA samples. These species are known to perform complete denitrification, to have a metabolic preference for nitrate as an electron acceptor, or are associated with denitrifying chemosymbionts (Bernhard et al., 2012; Glock et al., 2019; Piña-Ochoa et al., 2010). The presence of these species with metabolic adaptations for living in oxygen-depleted sediments further indicates the presence of no-analog low-oxygen conditions in our record.

These low-oxygen conditions in GoA that favor benthic foraminifera able to use nitrate-based metabolisms suggest that metazoan species would be extirpated during the dysoxic events. Median lethal dissolved oxygen concentrations from a study of benthic crabs, fish, bivalves and gastropods is ~1.2 ml/L (Vaquer-Sunyer & Duarte, 2008), which is far better oxygenated than we infer during dysoxic intervals. Laminated muds also occur in this record, particularly during the deglacial and at ~29, 36, and 43 ka (Davies et al., 2011; Penkrot et al., 2018), further suggesting that oxygen levels were occasionally low enough to exclude or reduce the activity of metazoans. Metazoan meiofauna (such as some nematodes) are more tolerant of low-oxygen conditions (Gallo & Levin, 2016), thus sediments under suboxic conditions, even if previously laminated during preceding dysoxia, may still have bioturbation due to the activities of those specialists.

4.4. Occurrence and Duration of Low Oxygen Events

Previous work in the GoA recognized low-oxygen events during the last deglacial using redox sensitive metals and selected index taxa from jumbo piston core and adjacent multicore (Davies et al., 2011; Praetorius et al., 2015) and using whole faunal assemblage analyses based on foraminiferal proxies at Site U1419 over the past 54 ka at much lower temporal resolution (Belanger et al., 2016). In the present study, using much higher resolution, we recognize low-oxygen events from whole assemblage analyses in interglacial, deglacial, and glacial conditions that are supported by enrichments in redox sensitive metals. While we base our faunally derived oxygenation history below on the >63 μm size fraction, the occurrence of events does not differ significantly when considering only the >125 μm size fraction (Figure 3).

4.4.1. Low-Oxygen Events in MIS 2 to the Holocene

Analyses of modern assemblages from the site indicate suboxic conditions, as expected from the site's position in the upper OMZ. Our high-resolution faunal analysis recognizes severe dysoxic events in the earliest Holocene and during the B/A interstadial. Between 14.7 and 13.8 ka, modified BDO values are sustained below 0.27 ml/L O_2 with redox metals values frequently in the upper 90th upper quantile of the data. This dysoxic event is followed by a better-oxygenated interval (BDO: 0.4–0.7 ml/L) from 13.2–11.8 ka, overlapping the YD. BDO estimates below 0.50 ml/L O_2 then reoccur in the early Holocene immediately following the YD along with elevated concentrations of Mo/Al and U/Al. In total, this deglacial low-oxygen interval lasts for ~4 ka in our GoA record, with a brief interruption during the YD, and corroborates previous work at the site (Davies et al., 2011; Du et al., 2018; Praetorius et al., 2015). Overall, redox sensitive metals corroborate the BDO estimates, especially during the extreme low-oxygen events in the deglacial.

Deglacial dysoxia during the B/A is also well recorded elsewhere in the North Pacific margin, but the proposed drivers vary (Moffitt et al., 2015). At ODP Site 1017, on the slope near Point Conception on the California margin, local productivity may have driven pore-water deoxygenation during the Bølling whereas incursion of low-oxygen intermediate waters may have contributed to dysoxia during the Allerød (Taylor et al., 2017). OMZ intensification on the Cascadia Margin also occurred during the B/A following a dramatic increase in primary productivity related to intense upwelling driven by changes in the California Undercurrent (McKay et al., 2005; Saravanan et al., 2020). High productivity has also been reported during the B/A in the Bering Sea and during the Allerød in the Okhotsk Sea (Max et al., 2014). The Bering and Okhotsk Seas are potential sources of NPIW during the glacial while the Okhotsk Sea is the primary source of NPIW in the modern (Knudson & Ravelo, 2015; Max et al., 2014; K. Ohkushi et al., 2016; Rella et al., 2012).

NPIW extends to the eastern parts of the North Pacific and low-oxygen conditions in Okhotsk Sea Intermediate Water (OSIW) influence the GoA and the eastern North Pacific margin (Max et al., 2014; K. Ohkushi et al., 2016). Local factors, such as organic carbon export, may then contribute to further deoxygenation of these source-waters.

Better-oxygenated intervals occur in our record during Heinrich Stadial (HS) 1 and the YD, consistent with previous GoA studies (Belanger et al., 2020; Davies et al., 2011; Du et al., 2018; Praetorius et al., 2015) and other North Pacific records. For example, increased oxygenation during HS1 in our record (17–15 ka, BDO > 0.99 ml/L) coincides with oxygenation >1.5 ml/L SBB (K. G. Cannariato et al., 1999; K. Ohkushi et al., 2013) and with a well-ventilated interval in the Okhotsk Sea (Max et al., 2014; K. Ohkushi et al. 2016) and Okinawa Trough (Zou et al., 2020). During the YD, intermediate depths on the eastern and western Pacific margins were also better-oxygenated (K. G. Cannariato et al., 1999; K. Cannariato & Kennett, 1999; Max et al., 2014; McKay et al., 2005; Taylor et al., 2017; Tetard et al., 2017; Zou et al., 2020). This relaxation of severe low-oxygen conditions is consistent with enhanced NPIW ventilation during the YD suggested by records near Hokkaido, Japan (Ivanochko & Pedersen, 2004; K. Ohkushi et al., 2016; Shibahara et al., 2007). Thus, better ventilation and decreased biological productivity during colder periods in the OSIW had broad effects on oxygenation in the GoA and California margin (K. Ohkushi et al., 2016; Shibahara et al., 2007). However, a decrease in primary productivity locally may also contribute to the increase in oxygenation on the California margin (Taylor et al., 2017).

Following the YD, oxygenation declined in GoA during the early Holocene (11.2–10.9 ka). A similarly timed low-oxygen event occurred near Vancouver Island from ~11–10 ka, potentially driven by decreased ventilation and increased productivity (McKay et al., 2005). In addition, dysoxic foraminifera increased in abundance during the early Holocene along the California margin to Baja California and in the western subtropical North Pacific (K. Cannariato and Kennett, 1999; Tetard et al., 2017; Zou et al., 2020), suggesting this low-oxygen event was also widespread. After this early Holocene deoxygenation, suboxic conditions dominate the remainder of our GoA record as evinced by generally higher DCA Axis 1 scores and lower BDO estimates (0.55–0.80 ml/L). Mo/Al and U/Al values in our record are also generally low (<80th upper quantile) during the Holocene, supporting oxygenation levels above the threshold accumulation for these metals. California margin slope Site ODP 1017, also increased in oxygenation after early Holocene dysoxia, while sites in the SBB, Baja California, and Sea of Japan remained as dysoxic as during the B/A (K. G. Cannariato et al., 1999; K. Cannariato and Kennett, 1999; K. Ohkushi et al., 2013; Shibahara et al., 2007; Tetard et al., 2017). Therefore, the GoA has a Holocene oxygenation history more similar to slope sites elsewhere in the North Pacific as compared to sites from more restricted basins, suggesting that local processes drive the maintenance of dysoxia at those sites. Previous work in the SBB and the California margin also suggests local changes in productivity become a more prominent control of oxygenation during the Holocene (Ivanochko & Pedersen, 2004).

4.4.2. Dysoxia During the Last Glacial

Long sedimentary records extending to MIS 3 that permit high-resolution analyses are generally lacking in the higher latitudes of the eastern North Pacific unlike more southern sites. In our ~54 kyr-long GoA record, faunal DCA Axis 1 scores and our modified BDO estimates suggest better-oxygenated background conditions during the glacial than during the Holocene. Similarly, on the California margin paleo-oxygen records based on foraminiferal proxies indicate better oxygenation in glacial times than in MIS 1 and 2 (K. G. Cannariato et al., 1999; K. Cannariato and Kennett, 1999; K. Ohkushi et al., 2013; Tetard et al., 2017). Thus, our paleo-oxygen reconstruction is overall consistent with lower-latitude foraminiferal records.

Despite the better-oxygenated background conditions of the glacial, we reconstruct three dysoxic events at 36.9–36.8 ka, 44–43.9 ka, and 46.7–45.7 ka that have BDO estimates <0.5 ml/L in more than one sample and are corroborated by enriched redox sensitive metals. Co-registered faunal assemblages and redox-sensitive metal concentrations also support shorter duration dysoxic events registered in single samples (Figure 3). BDO estimates suggest these MIS 3 dysoxic events are as low-oxygen as those in the better-studied deglacial and early Holocene (Figure 5). A lower-resolution U1419 record of biomarkers for the anaerobic oxidation of ammonium has a glacial high at ~46 ka, which corresponds with our longest period of dysoxia in MIS 3, and a lesser peak at ~29 ka coincident with a single-sample dysoxic event we detect, suggesting that water column oxygenation was also lowest during these intervals (Zindorf et al., 2020). While potential

uncertainties in age models make it difficult to directly align these events with those of other regions, similarly timed short-lived decreases in oxygenation occur in Baja California and the SBB where they appear to coincide with Daansgard-Oeschger (D-O) events and interstadials (K. G. Cannariato et al., 1999; Tetard et al., 2017). Thus, it is likely that these glacial-age low-oxygen events reported at lower latitudes occurred throughout the North Pacific Margin, including at subarctic latitudes. In addition, high-productivity events are recorded in the Bering Sea during MIS 3 that are also similar in timing to D-O events (Schlung et al., 2013), thus these shorter-term glacial events in GoA may also be influenced by productivity as hypothesized for the B/A dysoxic event and suggested by the high relative abundances of phytodetritus-sensitive species prior to the low-oxygen events (Figure 2).

Given many of these glacial dysoxic events in GoA lasted no longer than ~100–400 years based upon the ages of adjacent samples in which faunas indicate suboxic to weakly hypoxic conditions and redox metals are not enriched, it is clear that high-resolution sampling is necessary to capture these environmental changes. Given that our sample spacing exceeds 100 years in ~ 60% of cases, it is likely that our reconstruction also omits some low oxygen events recognized elsewhere in the North Pacific and certainly omits events that are shorter in duration than 100 years. For example, SBB records capture 9 dysoxic events from ~22 to 45 ka (K. Cannariato and Kennett, 1999), however our GoA record captures 6 events over the same interval. In addition, short-lived low-oxygen events are susceptible to bioturbation, which could have obscured the low-oxygen signal in the faunal record, and to oxic burn down of redox sensitive metals, which would remove this chemical tracer of low-oxygen (Zheng et al., 2002).

4.5. Rates of Faunal and Oxygenation Changes

While consecutive samples are typically similar to each other in their faunal composition given the high resolution of our sampling, changes in DCA Axis 1 scores exceeding 1 SD/100 years do occur between sequential adjacent samples, suggesting that changes in faunal composition can occur quite rapidly (Figure 5). Re-analysis considering potential down-slope transport suggested by the modern analog comparisons yield similar rates, thus the occurrence of downslope transport cannot explain the rapid changes in oxygenation conditions. Further, independent evidence for sedimentary transport at this site for the last ~54 ka is unreported. Changes in grain size and faunal composition could instead reflect in situ changes in environmental changes expected with influx of ice-rafted debris during glacial melting or blockage of fjords as glaciers retreat (Davies et al., 2011; Penkrot et al., 2018).

Systematic biases in the BDO equation imply that calculations of the rate of change from well-oxygenated conditions to low-oxygen conditions will be underestimates. Despite this shortcoming, we find multiple rapid changes in BDO values exceeding 0.5 ml/L per 100 years, even after accounting for potential downslope transport. Uncertainty in the age model can also affect our calculations of rates; however, any errors due to interpolation between the high-resolution radiocarbon data points should have an equal likelihood of decreasing rates as increasing them. Thus, it is likely that biologically significant changes in oxygenation can occur on decadal to centennial timescales in the upper OMZ of the GoA.

5. Conclusions

Cross-validated faunal and geochemical proxies reveal dysoxic and suboxic intervals during glacial, deglacial and interglacial times in GoA. Our quantitative paleo-oxygen reconstructions using total benthic foraminiferal assemblages, rather than index taxa, are robust to size fraction differences and suggest that the larger size fraction is sufficient for reconstructing paleo-oxygenation. Comparisons between modern and fossil assemblages demonstrate that oxygenation in the upper OMZ in GoA was lower than anywhere in the modern GoA during the last deglacial and during three distinct intervals in MIS 3. Thus, an intense OMZ can develop in this subarctic region during both glacial and interglacial times, similar to lower latitudes and restricted basins elsewhere in the North Pacific. Similarities in the timing of events across the North Pacific suggests a common, basin-wide driver of oxygenation, perhaps related to warm climate events, enhanced productivity around the basin margins, or changing intermediate-depth ventilation. While many of the low-oxygen events in GoA are geologically brief, transitions between oxic and suboxic conditions, or

between suboxic and dysoxic conditions, can occur in less than 100 years, rapidly enough to have ecological consequences. Quantitative estimates of oxygenation such as these from benthic foraminiferal assemblages are important for modeling of future changes in OMZs and their ecosystem effects.

Data Availability Statement

Data are archived with the NOAA World Data Service for Paleoclimatology at https://www.ncdc.noaa.gov/paleo/study/31412.

Acknowledgments
This work was supported by NSF 1502746 and 1801511 to CLB and NSF 1360894 and 1502754 to ACM. We thank Jesse Muratli from the W. M. Keck Collaboratory for Plasma Spectrometry of Oregon State University for assistance with digesting sediment samples and analyzing metal concentrations. We thank June Padman, Jennifer McKay, and Andy Ross for assistance with stable isotope analyses. Perry Chesebro, Ozlem Orhun, Adrian Sweeney, and Christopher Schiller at SDSMT and Pablo Cavazos, Calie Payne at TAMU assisted with fossil sample preparation. We are also grateful to two anonymous reviewers whose suggestions improved this manuscript.

References

Addison, J. A., Finney, B. P., Dean, W. E., Davies, M. H., Mix, A. C., Stoner, J. S., & Jaeger, J. M. (2012). Productivity and sedimentary $\delta^{15}N$ variability for the last 17,000 years along the northern Gulf of Alaska continental slope. *Paleoceanography and Paleoceanography*, *27*, PA1206. https://doi.org/10.1029/2011PA002161

Alve, E. (2003). A common opportunistic foraminiferal species as an indicator of rapidly changing conditions in a range of environments. *Estuarine, Coastal and Shelf Science*, *57*(3), 501–514. https://doi.org/10.1016/S0272-7714(02)00383-9

Belanger, C. L., Orhun, O. G., & Schiller, C. M. (2016). Benthic foraminiferal faunas reveal transport dynamics and no-analog environments on a glaciated margin (Gulf of Alaska). *Palaeogeography, Palaeoclimatology, Palaeoecology*, *454*, 54–64. https://doi.org/10.1016/j.palaeo.2016.04.032

Belanger, C. L., Du, J., Payne, C. R., & Mix, A. C. (2020). North Pacific deep-sea ecosystem responses reflect post-glacial switch to pulsed export productivity, deoxygenation, and destratification. *Deep Sea Research Part I: Oceanographic Research Papers*, *164*, 103341. https://doi.org/10.1016/j.dsr.2020.103341

Belanger, C. L., & Villarosa Garcia, M. (2014). Differential drivers of benthic foraminiferal and molluscan community composition from a multivariate record of early Miocene environmental change. *Paleobiology*, *40*(3), 398–416. https://doi.org/10.1666/13019

Bergen, F. W., & O'Neil, P. (1979). Distribution of Holocene foraminifera in the Gulf of Alaska. *Journal of Paleontology*, *53*(6), 1267–1292.

Bernhard, J. M., Casciotti, K. L., McIlvin, M. R., Beaudoin, D. J., Visscher, P. T., & Edgcomb, V. P. (2012). Potential importance of physiologically diverse benthic foraminifera in sedimentary nitrate storage and respiration. *Journal of Geophysical Research*, *117*, G03002. https://doi.org/10.1029/2012JG001949

Bograd, S. J., Castro, C. G., Di Lorenzo, E., Palacios, D. M., Bailey, H., Gilly, W., & Chavez, F. P. (2008). Oxygen declines and the shoaling of the hypoxic boundary in the California Current. *Geophysical Research Letters*, *35*, L12607. https://doi.org/10.1029/2008GL034185

Bouchet, V. M. P., Alve, E., Rygg, B., & Telford, R. J. (2012). Benthic foraminifera provide a promising tool for ecological quality assessment of marine waters. *Ecological Indicators*, *23*, 66–75. https://doi.org/10.1016/j.ecolind.2012.03.011

Bubenshchikova, N., Nürnberg, D., & Tiedemann, R. (2015). Variations of Okhotsk Sea oxygen minimum zone: Comparison of foraminiferal and sedimentological records for latest MIS 12–11c and latest MIS 2–1. *Marine Micropaleontology*, *121*, 52–69. https://doi.org/10.1016/j.marmicro.2015.09.004

Bush, A. M., & Brame, R. I. (2010). Multiple paleoecological controls on the composition of marine fossil assemblages from the Frasnian (Late Devonian) of Virginia, with a comparison of ordination methods. *Paleobiology*, *36*(4), 573–591.

Buzas, M. (1990). Another look at confidence limits for species proportions. *Journal of Paleontology*, *64*(5), 842–843. https://doi.org/10.1017/S002233600001903X

Calvert, S. E., & Pedersen, T. F. (1993). Geochemistry of recent oxic and anoxic marine sediments: Implications for the geological record. *Marine Geology*, *113*(1–2), 67–3227.

Cannariato, K. G., Kennett, J. P., & Behl, R. J. (1999). Biotic response to late quaternary rapid climate switches in Santa Barbara Basin: Ecological and evolutionary implications. *Geology*, *27*(1), 63–66.

Cannariato, K., & Kennett, J. (1999). Climatically related millennial-scale fluctuations in strength of California margin oxygen-minimum zone during the past 60 k.y. *Geology*, *27*, 975–978.

Carlson, P. R. (1989). Seismic reflection characteristics of glacial and glacimarine sediment in the Gulf of Alaska and adjacent fjords. *Marine Geology*, *85*(2–4), 391–416.

Cartapanis, O., Tachikawa, K., & Bard, E. (2011). Northeastern Pacific oxygen minimum zone variability over the past 70 kyr: Impact of biological production and oceanic ventilation. *Paleoceanography*, *26*, PA4208. https://doi.org/10.1029/2011PA002126

Cedhagen, T. (1991). Retention of chloroplasts and bathymetric distribution in the sublittoral foraminifera *Nonionellina labradorica*. *Ophelia*, *33*, 17–30. https://doi.org/10.1080/00785326.1991.10429739

Childers, A. R., Whitledge, T. E., & Stockwell, D. A. (2005). Seasonal and interannual variability in the distribution of nutrients and chlorophyll a across the Gulf of Alaska shelf: 1998–2000. *Deep Sea Research Part II: Topical Studies in Oceanography*, *52*(1), 193–216. https://doi.org/10.1016/j.dsr2.2004.09.018

Correa-Metrio, A., Bush, M. B., Cabrera, K. R., Sully, S., Brenner, M., Hodell, D. A., et al. (2012). Rapid climate change and no-analog vegetation in lowland Central America during the last 86,000 years. *Quaternary Science Reviews*, *38*, 63–75. https://doi.org/10.1016/j.quascirev.2012.01.025

Crusius, J., Calvert, S., Pedersen, T., & Sage, D. (1996). Rhenium and molybdenum enrichments in sediments as indicators of oxic, suboxic and sulfidic conditions of deposition. *Earth and Planetary Science Letters*, *145*, 65–78. https://doi.org/10.1016/S0012-821X(96)00204-X

Davies, M. H., Mix, A. C., Stoner, J. S., Addison, J. A., Jaeger, J., Finney, B., & Wiest, J. (2011). The deglacial transition on the southeastern Alaska Margin: Meltwater input, sea level rise, marine productivity, and sedimentary anoxia. *Paleoceanography and Paleoclimatology*, *26*, PA2223. https://doi.org/10.1029/2010PA002051

Deutsch, C., Brix, H., Ito, T., Frenzel, H., & Thompson, L. (2011). Climate-forced variability of ocean hypoxia. *Science*, *333*(6040), 336–339. https://doi.org/10.1126/science.1202422

Diaz, R. J., & Rosenberg, R. (2008). Spreading dead zones and consequences for marine ecosystems. *Science*, *321*(5891), 926–929. https://doi.org/10.1126/science.1156401

Dobson, M. R., O'Leary, D., & Veart, M. (1998). Sediment delivery to the Gulf of Alaska: Source mechanisms along a glaciated transform margin. *Geological Society, London, Special Publications*, *129*(1), 43–66.

Du, J., Haley, B. A., Mix, A. C., Walczak, M. H., & Praetorius, S. K. (2018). Flushing of the deep Pacific Ocean and the deglacial rise of atmospheric CO_2 concentrations. *Nature Geoscience*, *11*(10), 749–755. https://doi.org/10.1038/s41561-018-0205-6

Echols, R. J., & Armentrout, J. M. (1980). Holocene foraminiferal distribution patterns on shelf and slope, Yakataga-Yakutat area, Northern Gulf of Alaska. *AAPG Bulletin*, *64*(3), 440–441.

Erdem, Z., & Schönfeld, J. (2017). Pleistocene to Holocene benthic foraminiferal assemblages from the Peruvian continental margin. *Palaeontologia Electronica*, *20.2*, 1–32. 20.2.35A. https://doi.org/10.26879/764

Forcino, F. L., Leighton, L. R., Twerdy, P., & Cahill, J. F. (2015). Reexamining sample size requirements for multivariate, abundance-based community research: When resources are limited, the research does not have to be. *PloS One*, *10*(6), e0128379. https://doi.org/10.1371/journal.pone.0128379

Fürsich, F. T., & Aberhan, M. (1990). Significance of time-averaging for palaeocommunity analysis. *Lethaia*, *23*(2), 143–152. https://doi.org/10.1111/j.1502-3931.1990.tb01355.x

Gallo, N. D., & Levin, L. A. (2016). Fish ecology and evolution in the world's oxygen minimum zones and implications of ocean deoxygenation. *Advances in Marine Biology*, *74*, 117–198. https://doi.org/10.1016/bs.amb.2016.04.001

Garcia, H. E., Boyer, T. P., Locarnini, R. A., Antonov, J. I., Mishonov, A. V., Baranova, O. K., et al. (2013). World ocean atlas 2013. Volume 3: Dissolved oxygen, apparent oxygen utilization, and oxygen saturation. In S. Levitus, & A. Mishonov (Eds.), NOAA Atlas NESDIS. Vol. 75 (pp. 27).

Gilly, W. F., Beman, J. M., Litvin, S. Y., & Robison, B. H. (2013). Oceanographic and biological effects of shoaling of the oxygen minimum zone. *Annual Review of Marine Science*, *5*, 393–420.

Glock, N., Roy, A.-S., Romero, D., Wein, T., Weissenbach, J., Revsbech, N. P., et al. (2019). Metabolic preference of nitrate over oxygen as an electron acceptor in foraminifera from the Peruvian oxygen minimum zone. *Proceedings of the National Academy of Sciences*, *116*(8), 2860–2865. https://doi.org/10.1073/pnas.1813887116

Gooday, A. J. (1993). Deep-sea benthic foraminiferal species which exploit phytodetritus: Characteristic features and controls on distribution. *Marine Micropaleontology*, *22*(3), 187–205. https://doi.org/10.1016/0377-8398(93)90043-W

Gooday, A. J., & Goineau, A. (2019). The contribution of fine sieve fractions (63–150 μm) to foraminiferal abundance and diversity in an area of the Eastern Pacific Ocean licensed for polymetallic nodule exploration. *Frontiers in Marine Science*, *6*, 114. https://doi.org/10.3389/fmars.2019.00114

Gooday, A. J., & Jorissen, F. J. (2012). Benthic foraminiferal biogeography: Controls on global distribution patterns in deep-water settings. *Annual Review of Marine Science*, *4*(1), 237–262. https://doi.org/10.1146/annurev-marine-120709-142737

Goslee, S. C., & Urban, D. L. (2007). The ecodist package for dissimilarity-based analysis of ecological data. *Journal of Statistical Software*, *22*(7), 1–19.

Gray, W. R., Rae, J. W. B., Wills, R. C. J., Shevenell, A. E., Taylor, B., Burke, A., et al. (2018). Deglacial upwelling, productivity and CO2 outgassing in the North Pacific Ocean. *Nature Geoscience*, *11*(5), 340–344. https://doi.org/10.1038/s41561-018-0108-6

Gulick, S. P. S., Jaeger, J. M., Mix, A. C., Asahi, H., Bahlburg, H., Belanger, C. L., et al. (2015). Mid-Pleistocene climate transition drives net mass loss from rapidly uplifting St. Elias Mountains, Alaska. *Proceedings of the National Academy of Sciences*, *112*(49), 15042–15047. https://doi.org/10.1073/pnas.1512549112

Helly, J. J., & Levin, L. A. (2004). Global distribution of naturally occurring marine hypoxia on continental margins. *Deep Sea Research Part I: Oceanographic Research Papers*, *51*(9), 1159–1168

Ito, T., Minobe, S., Long, M. C., & Deutsch, C. (2017). Upper ocean O_2 trends: 1958–2015. *Geophysical Research Letters*, *44*(9), 4214–4223.

Ivanochko, T. S., & Pedersen, T. F. (2004). Determining the influences of late quaternary ventilation and productivity variations on Santa Barbara Basin sedimentary oxygenation: A multi-proxy approach. *Quaternary Science Reviews*, *23*(3), 467–480. https://doi.org/10.1016/j.quascirev.2003.06.006

Jaccard, S. L., & Galbraith, E. D. (2012). Large climate-driven changes of oceanic oxygen concentrations during the last deglaciation. *Nature Geoscience*, *5*(2), 151–156. https://doi.org/10.1038/ngeo1352

Jaccard, S. L., & Galbraith, E. D. (2013). Direct ventilation of the North Pacific did not reach the deep ocean during the last deglaciation. *Geophysical Research Letters*, *40*(1), 199–203. https://doi.org/10.1029/2012GL054118

Jaeger, J. M., Gulick, S. P. S., LeVay, L. J., Asahi, H., Bahlburg, H., Belanger, C. L., et al. (2014). *Proceedings of the Integrated Ocean Drilling Program Vol. 314: Expedition reports Southern Alaska margin*. Integrated Ocean Drilling Program. http://publications.iodp.org/proceedings/341/341toc.htm

Jochum, K. P., Weis, U., Schwager, B., Stoll, B., Wilson, S. A., Haug, G. H., et al. (2016). Reference values following ISO guidelines for frequently requested rock reference materials. *Geostandards and Geoanalytical Research*, *40*(3), 333–350. https://doi.org/10.1111/j.1751-908X.2015.00392.x

Jorissen, F. J., Fontanier, C., & Thomas, E. (2007). Paleoceanographical proxies based on deep-sea benthic foraminiferal assemblage characteristics. In C. Hillaire–Marcel, & A. De Vernal (Eds.), Proxies in late cenozoic paleoceanography. Vol. 1 (pp. 263–325). https://doi.org/10.1016/S1572-5480(07)01012-3

Keeling, R. F., Körtzinger, A., & Gruber, N. (2010). Ocean deoxygenation in a warming world. *Annual Review of Marine Science*, *2*(1), 199–229. https://doi.org/10.1146/annurev.marine.010908.163855

Klinkhammer, G. P., & Palmer, M. R. (1991). Uranium in the oceans: Where it goes and why. *Geochimica et Cosmochimica Acta*, *55*(7), 1799–1806. https://doi.org/10.1016/0016-7037(91)90024-Y

Knudson, K. P., & Ravelo, A. C. (2015). North Pacific Intermediate Water circulation enhanced by the closure of the Bering Strait. *Paleoceanography*, *30*(10), 1287–1304. https://doi.org/10.1002/2015PA002840

Li, G., Rashid, H., Zhong, L., Xu, X., Yan, W., & Chen, Z. (2018). Changes in deep water oxygenation of the south China sea since the last glacial period. *Geophysical Research Letters*, *45*(17), 9058–9066. https://doi.org/10.1029/2018GL078568

Max, L., Lembke-Jene, L., Riethdorf, J. R., Tiedemann, R., Nürnberg, D., Kühn, H., & MacKensen, A. (2014). Pulses of enhanced north Pacific intermediate water ventilation from the Okhotsk Sea and Bering Sea during the last deglaciation. *Climate of the Past*, *10*(2), 591–605. https://doi.org/10.5194/cp-10-591-2014

McCune, B., Grace, J. B. J. B., Urban, D. L., & Beach, G. (2002). Analysis of ecological communities. MjM Software Design (Vol. 28). Gleneden Beach, OR.

McKay, J. L., Pedersen, T. F., & Southon, J. (2005). Intensification of the oxygen minimum zone in the northeast Pacific off Vancouver Island during the last deglaciation: Ventilation and/or export production? *Paleoceanography*, *20*, PA4002. https://doi.org/10.1029/2003PA000979

McManus, J., Berelson, W., Severmann, S., Poulson, R., Hammond, D., Klinkhammer, G., & Holm, C. (2006). Molybdenum and uranium geochemistry in continental margin sediments: Paleoproxy potential. *Geochimica et Cosmochimica Acta*, *70*, 4643–4662. https://doi.org/10.1016/j.gca.2006.06.1564

Mix, A. C., Lund, D. C., Pisias, N. G., Bodén, P., Bornmalm, L., Lyle, M., & Pike, J. (1999). Rapid climate oscillations in the northeast Pacific during the last deglaciation reflect Northern and Southern Hemisphere sources. *Geophysical Monograph-American Geophysical Union*, *112*, 127–148.

Moffitt, S. E., Hill, T. M., Ohkushi, K., Kennett, J. P., & Behl, R. J. (2014). Vertical oxygen minimum zone oscillations since 20 ka in Santa Barbara Basin: A benthic foraminiferal community perspective. *Paleoceanography*, *29*(1), 44–57. https://doi.org/10.1002/2013PA002483

Moffitt, S. E., Moffitt, R. A., Sauthoff, W., Davis, C. V., Hewett, K., & Hill, T. M. (2015). Paleoceanographic insights on recent oxygen minimum zone expansion: Lessons for modern oceanography. *PloS One*, *10*(1), e0115246. https://doi.org/10.1371/journal.pone.0115246

Molnia, B. F. (1983). Subarctic glacial-marine sedimentation: A model. In B. F. Molnia (Ed.), *Glacial-marine sedimentation* (pp. 95–144). Boston, MA: Springer US. https://doi.org/10.1007/978-1-4613-3793-5_2

Muratli, J., Chase, Z., Mix, A., & McManus, J. (2010). Increased glacial-age ventilation of the Chilean margin by Antarctic intermediate water. *Nature Geoscience*, *3*, 23–26.

Muratli, J. M., McManus, J., Mix, A., & Chase, Z. (2012). Dissolution of fluoride complexes following microwave-assisted hydrofluoric acid digestion of marine sediments. *Talanta*, *89*, 195–200.

Murray, J. W. (2001). The niche of benthic foraminifera, critical thresholds and proxies. *Marine Micropaleontology*, *41*(1), 1–7. https://doi.org/10.1016/S0377-8398(00)00057-8

Ohkushi, K., Hara, N., Ikehara, M., Uchida, M., & Ahagon, N. (2016). Intensification of North Pacific intermediate water ventilation during the younger Dryas. *Geo-Marine Letters*, *36*, 353–360. https://doi.org/10.1007/s00367-016-0450-x

Ohkushi, K. I., Itaki, T., & Nemoto, N. (2003). Last Glacial–Holocene change in intermediate-water ventilation in the Northwestern Pacific. *Quaternary Science Reviews*, *22*, 1477–1484.

Ohkushi, K., Kennett, J. P., Zeleski, C. M., Moffitt, S. E., Hill, T. M., Robert, C., et al. (2013). Quantified intermediate water oxygenation history of the NE pacific: A new benthic foraminiferal record from Santa Barbara Basin. *Paleoceanography*, *28*(3), 453–467. https://doi.org/10.1002/palo.20043

Oksanen, J., Blanchet, F. G., Friendly, M., Kindt, R., Legendre, P., McGlinn, D., et al. (2017). *Vegan: Community ecology package*. Retrieved from cran.r-project.org/package=vegan

Paulmier, A., & Ruiz-Pino, D. (2009). Oxygen minimum zones (OMZs) in the modern ocean. *Progress in Oceanography*, *80*(3), 113–128. https://doi.org/10.1016/j.pocean.2008.08.001

Penkrot, M. L., Jaeger, J. M., Cowan, E. A., St-Onge, G., & Levay, L. (2018). Multivariate modeling of glacimarine lithostratigraphy combining scanning XRF, multisensory core properties, and CT imagery: IODP site U1419. *Geosphere*, *14*(4), 1935–1960. https://doi.org/10.1130/GES01635.1

Pierce, S. D., Barth, J. A., Shearman, R. K., & Erofeev, A. Y. (2012). Declining oxygen in the northeast pacific. *Journal of Physical Oceanography*, *42*(3), 495–501.

Piña-Ochoa, E., Høgslund, S., Geslin, E., Cedhagen, T., Revsbech, N. P., Nielsen, L. P., et al. (2010). Widespread occurrence of nitrate storage and denitrification among Foraminifera and Gromiida. *Proceedings of the National Academy of Sciences*, *107*(3), 1148. LP – 1153. https://doi.org/10.1073/pnas.0908440107

Praetorius, S. K., Mix, A. C., Walczak, M. H., Wolhowe, M. D., Addison, J. A., & Prahl, F. G. (2015). North Pacific deglacial hypoxic events linked to abrupt ocean warming. *Nature*, *527*, 362–366. https://doi.org/10.1038/nature15753

R Core Team (2016). *R: A language and environment for Statistical computing*. Vienna, Austria. Retrieved from www.r-project.org/

Rella, S. F., Tada, R., Nagashima, K., Ikehara, M., Itaki, T., Ohkushi, K., et al. (2012). Abrupt changes of intermediate water properties on the northeastern slope of the Bering Sea during the last glacial and deglacial period. *Paleoceanography*, *27*(3). https://doi.org/10.1029/2011PA002205

Saravanan, P., Gupta, A. K., Zheng, H., Rai, S. K., & Panigrahi, M. K. (2020). Changes in deep-sea oxygenation in the northeast Pacific Ocean during 32–10 ka. *Geophysical Research Letters*, *47*(11), e2019GL086613. https://doi.org/10.1029/2019GL086613

Scarponi, D., & Kowalewski, M. (2004). Stratigraphic paleoecology: Bathymetric signatures and sequence overprint of mollusk associations from upper Quaternary sequences of the Po Plain, Italy. *Geology*, *32*(11), 989–992.

Schlitzer, R. (2018). *Ocean data view*. Retrieved from https://odv.awi.de

Schlung, S. A., Ravelo, A. C., Aiello, I. W., Andreasen, D. H., Cook, M. S., Drake, M., et al. (2013). Millennial-scale climate change and intermediate water circulation in the Bering Sea from 90 ka: A high-resolution record from IODP site U1340. *Paleoceanography*, *28*(1), 54–67. https://doi.org/10.1029/2012PA002365

Schmidtko, S., Stramma, L., & Visbeck, M. (2017). Decline in global oceanic oxygen content during the past five decades. *Nature*, *542*, 335–339. https://doi.org/10.1038/nature21399

Schmiedl, G., Mitschele, A., Beck, S., Emeis, K.-C., Hemleben, C., Schulz, H., et al. (2003). Benthic foraminiferal record of ecosystem variability in the eastern Mediterranean Sea during times of sapropel S5 and S6 deposition. *Palaeogeography, Palaeoclimatology, Palaeoecology*, *190*, 139–164. https://doi.org/10.1016/S0031-0182(02)00603-X

Schönfeld, J., Alve, E., Geslin, E., Jorissen, F., Korsun, S., & Spezzaferri, S. (2012). The FOBIMO (FOraminiferal BIo-MOnitoring) initiative—Towards a standardized protocol for soft-bottom benthic foraminiferal monitoring studies. *Marine Micropaleontology*, 1–13.94–95. https://doi.org/10.1016/j.marmicro.2012.06.001

Schroeder, C. J., Scott, D. B., & Medioli, F. S. (1987). Can smaller benthic foraminifera be ignored in paleoenvironmental analyses? *Journal of Foraminiferal Research*, *17*(2), 101–105. https://doi.org/10.2113/gsjfr.17.2.101

Sen Gupta, B. K., Shin, I. C., & Wendler, S. T. (1987). Relevance of specimen size in distribution studies of deep-sea benthic foraminifera. *PALAIOS*, *2*(4), 332–338. https://doi.org/10.2307/3514758

Shibahara, A., Ohkushi, K., Kennett, J. P., & Ikehara, K. (2007). Late quaternary changes in intermediate water oxygenation and oxygen minimum zone, northern Japan: A benthic foraminiferal perspective. *Paleoceanography*, *22*, PA3213. https://doi.org/10.1029/2005PA001234

Stabeno, P. J., Bond, N. A., Hermann, A. J., Kachel, N. B., Mordy, C. W., & Overland, J. E. (2004). Meteorology and oceanography of the northern Gulf of Alaska. *Continental Shelf Research*, *24*(7–8), 859–897.

Sun, X., Corliss, B. H., Brown, C. W., & Showers, W. J. (2006). The effect of primary productivity and seasonality on the distribution of deep-sea benthic foraminifera in the North Atlantic. *Deep Sea Research Part I: Oceanographic Research Papers*, *53*(1), 28–47. https://doi.org/10.1016/j.dsr.2005.07.003

Takahashi, K., Ravelo, A. C., & Okazaki, Y. (2016). Introduction to Pliocene–Pleistocene paleoceanography of the Bering Sea. *Deep Sea Research Part II: Topical Studies in Oceanography*, *125–126*, 1–7. https://doi.org/10.1016/j.dsr2.2016.03.001

Taylor, M. A., Hendy, I. L., & Chappaz, A. (2017). Assessing oxygen depletion in the Northeastern Pacific Ocean during the last deglaciation using I/Ca ratios from multiple benthic foraminiferal species. *Paleoceanography*, *32*(8), 746–762. https://doi.org/10.1002/2016PA003062

Tetard, M., Licari, L., & Beaufort, L. (2017). Oxygen history off Baja California over the last 80 kyr: A new foraminiferal-based record. *Paleoceanography*, *32*, 246–264. https://doi.org/10.1002/2016PA003034

Tribovillard, N., Algeo, T. J., Lyons, T., & Riboulleau, A. (2006). Trace metals as paleoredox and paleoproductivity proxies: An update. *Chemical Geology*, *232*(1), 12–32. https://doi.org/10.1016/j.chemgeo.2006.02.012

van Geen, A., Zheng, Y., Bernhard, J. M., Cannariato, K. G., Carriquiry, J., Dean, W. E., et al. (2003). On the preservation of laminated sediments along the western margin of North America. *Paleoceanography*, *18*, 1098. https://doi.org/10.1029/2003PA000911

Vaquer-Sunyer, R., & Duarte, C. M. (2008). Thresholds of hypoxia for marine biodiversity. *Proceedings of the National Academy of Sciences*, *105*(40), 15452–15457. https://doi.org/10.1073/pnas.0803833105

Walczak, M. H., Mix, A. C., Cowan, E. A., Fallon, S., Fifield, L. K., Du, J., et al. (2020). Phasing of millennial-scale climate variability in the pacific and Atlantic oceans. *Science*, *370*, 716–720. https://doi.org/10.1126/science.aba7096

Weinkauf, M., & Milker, Y. (2018). The effect of size fraction in analyses of benthic foraminiferal assemblages: A case study comparing assemblages from the >125 and >150 μm size fractions. *Frontiers in Earth Science*, *6*(37). https://doi.org/10.3389/feart.2018.00037

Whitney, F. A., Freeland, H. J., & Robert, M. (2007). Persistently declining oxygen levels in the interior waters of the eastern subarctic Pacific. *Progress in Oceanography*, *75*(2), 179–199. https://doi.org/10.1016/j.pocean.2007.08.007

Zheng, Y., Anderson, R. F., van Geen, A., & Fleisher, M. Q. (2002). Remobilization of authigenic uranium in marine sediments by bioturbation. *Geochimica et Cosmochimica Acta*, *66*(10), 1759–1772. https://doi.org/10.1016/S0016-7037(01)00886-9

Zheng, Y., Anderson, R. F., van Geen, A., & Kuwabara, J. (2000). Authigenic molybdenum formation in marine sediments: A link to pore water sulfide in the Santa Barbara Basin. *Geochimica et Cosmochimica Acta*, *64*(24), 4165–4178. https://doi.org/10.1016/S0016-7037(00)00495-6/10.1016/S0016-7037(00)00495-6

Zindorf, M., Rush, D., Jaeger, J., Mix, A., Penkrot, M. L., Schnetger, B., et al. (2020). Reconstructing oxygen deficiency in the glacial Gulf of Alaska: Combining biomarkers and trace metals as paleo-redox proxies. *Chemical Geology*, *558*. 119864. https://doi.org/10.1016/j.chemgeo.2020.119864

Zou, J., Shi, X., Zhu, A., Kandasamy, S., Gong, X., Lembke-Jene, L., et al. (2020). Millennial-scale variations in sedimentary oxygenation in the western subtropical North Pacific and its links to North Atlantic climate. *Climate of the Past*, *16*(1), 387–407. https://doi.org/10.5194/cp-16-387-2020